**On the Role of Computational Thermodynamics
in Research and Development of AOD and CRC processes**

E e t u - P e k k a   H e i k k i n e n

University of Oulu Graduate School

Department of Process and Environmental Engineering

Laboratory of Process Metallurgy

Doctoral Thesis

On the Role of Computational Thermodynamics
in Research and Development of AOD and CRC processes

Eetu-Pekka Heikkinen

Laboratory of Process Metallurgy

Department of Process and Environmental Engineering

University of Oulu Graduate School

ACADEMIC DISSERTATION

to be presented with the assent of the Faculty of Technology, University of Oulu,

for public discussion in Auditorium L10 on Linnanmaa on September 13th, 2013

at 12.00.

Principal supervisor

Professor Timo Fabritius, University of Oulu, Finland

Pre-examiners

PhD Paavo Hooli, Outokumpu Stainless Oy, Finland

Professor emeritus Heikki Jalkanen, Aalto University, Finland

Opponent

Professor Bo Björkman, Luleå University of Technology, Sweden

To Kaisa

Preface

This thesis was written during the first two weeks of March 2013 and finalized based on pre-examiners' comments in early June 2013. However, the research presented in this thesis is executed during a much longer period of time. I have studied the things presented in this thesis for the last fifteen years, during which I have used computational thermodynamics as a tool in various research projects (some of which are not related to stainless steelmaking at all) and taught thermodynamics for students of metallurgy, process engineering and environmental engineering in several basic and advanced courses. During these years I have received partial funding, grants and prizes from the Finnish Funding Agency for Technology and Innovation, steel companies Outokumpu and Ruukki, foundations of Outokumpu Oyj and Tauno Tönning as well as Finnish Foundation for Technology Promotion, all of which are kindly acknowledged.

This thesis includes six original papers that I have had a pleasure to write together with Timo Fabritius, Tommi Kokkonen, Jouko Härkki, Jaana Riipi, Pentti Kupari, Aki Kärnä, Topi Ikäheimonen, Olli Mattila and Ville-Valtteri Visuri, all of which deserve big thanks for their contribution to the papers. Additionally, I want to thank those whose contribution has also helped to write these papers: Juha Roininen, Hannu Makkonen, Veikko Juntunen, Mika Järvinen, Arto Rousu, Jari Savolainen, Petri Sulasalmi, Petri Mure, Jukka Hiltunen, Jyrki Heino as well as operators of the CRC process and the personnel of the analytical laboratory of the Outokumpu Stainless Tornio works.

I also want to thank Paavo Hooli and Heikki Jalkanen for being pre-examiners for this thesis and giving me valuable comments, which helped me to improve the text considerably.

Many persons have inspired me in my work (in research as well as in education) and increased my interest towards process metallurgy and thermodynamics with their teachings, discussions, writings or just by being an example to follow. At this point I want to highlight the role of Pekka Taskinen, Markku Kytö, Päivi Mannila, Martti Veistaro, Matti Seppänen, Kari Helelä, Veikko Heikkinen, current and former members of 'Metallurgian VAT', Pär Jönsson, Kari Heiskanen, Jenni Koponen, Lauri Holappa, Janne Palosaari, Matti Luomala, Helena Erkkilä, Pekka Tanskanen, Riku Mattila, Esa Virtanen, Timo Paananen, Tuomas Alatarvas, David Porter, Veikko Pohjola, Arja Sarpola, Juha Jaako, Suzy McAnsh, Juha Ahola, Asko Karjalainen, Päivi Tynjälä, Mari Murtonen, Sanna Vehviläinen, always inspirational student

In theory, there is no difference between theory and practice.
In practice, there is no connection between theory and practice.

Heikkinen, Eetu-Pekka

On the role of computational thermodynamics in research and development of AOD and CRC processes

Faculty of Technology, University of Oulu, PO Box 4000. FI-90014 University of Oulu, Finland. Department of Process and Environmental Engineering, University of Oulu, PO Box 4300. FI-90014 University of Oulu, Finland.

Oulu, Finland

Abstract

Chemical reactions are an essential part of all metallurgical processes. Hence, computational thermodynamics, that makes it possible to study the spontaneities of chemical reactions, is one of the most important tools in metallurgical research and development.

Within this thesis and its supplements, the role of computational thermodynamics in the research and development of AOD and CRC processes used in the production of stainless steels has been analysed. In addition to the results of computational thermodynamics and their application in metallurgical practice, one purpose of this thesis has been to consider what is the role of computational thermodynamics and other tools of research and development as a link between metallurgical theory and practice. Furthermore, the consequences of this kind of analysis on research, development and education has been considered.

The cases presented in this thesis and its supplements focus on the oxidation of silicon, carbon and chromium in CRC process, on nitrogen solubility in stainless steel melts in AOD process, on metal-slag -equilibria in CRC process as well as on melting and solidification of AOD and CRC slags. These cases have been chosen to represent different kind of reactions (*i.e.* liquid-gas, liquid-liquid as well as liquid-solid reactions) taking place in the stainless steel refining processes.

Keywords: computational thermodynamics, metallurgical R&D, AOD process, CRC process, stainless steelmaking, engineering education.

Heikkinen, Eetu-Pekka
Termodynaamisen mallinnuksen roolista AOD- ja CRK-konvertterien tutkimus- ja kehitystyössä
Teknillinen tiedekunta, Oulun yliopisto, PL 4000, 90014 Oulun yliopisto.
Prosessi- ja ympäristötekniikan osasto. PL 4300. 90014 Oulun yliopisto.
Oulu.

Tiivistelmä

Kemialliset reaktiot ovat keskeisessä roolissa kaikissa metallurgisissa tuotantoprosesseissa. Sen vuoksi laskennallinen termodynamiikka, jonka avulla on mahdollista tarkastella reaktioiden spontaanisuutta, on yksi tärkeimmistä työkaluista metallurgisessa tutkimus- ja kehitystyössä.

Tässä työssä ja sen liitteissä on tarkasteltu laskennallisen termodynamiikan roolia ruostumattoman teräksen valmistuksessa käytettävien AOD- ja CRK-konvertterien tutkimus- ja kehitystyössä. Laskennallisella termodynamiikalla saavutettujen tutkimustulosten ja niiden käytännön sovellusten lisäksi työssä on tarkasteltu termodynamiikan - ja muiden tutkimusmenetelmien - roolia teoriaa ja käytäntöä yhdistävänä tekijänä. Lisäksi on arvioitu mitä vaikutuksia tällaisella lähestymistavalla on metallurgiaan käytännössä, tutkimuksessa ja opetuksessa.

Työssä esitellyt esimerkkitapaukset liittyvät piin, hiilen ja kromin hapettumisreaktioihin CRK-prosessissa, typen liukoisuuten ruostumattomissa terässulissa AOD-konvertterissa, metalli-kuona-tasapainoihin CRK-prosessissa sekä kuonien sulamis- ja jähmettymiskäyttäytymiseen AOD- ja CRK-prosesseissa. Esimerkkitapaukset on pyritty valitsemaan siten, että ne edustavat erilaisia teräksen valmistusprosesseissa esiintyviä reaktiotyyppejä eli sula-kaasu-, sula-sula- ja sula-kiinteä -reaktioita.

Avainsanat: laskennallinen termodynamiikka, metallurginen T&K, AOD-konvertteri, ferrokromikonvertteri, ruostumattoman teräksen valmistus, teknillinen koulutus.

List of original papers

I   Heikkinen, Eetu-Pekka, Fabritius, Timo, Kokkonen, Tommi & Härkki, Jouko. An experimental and computational study on the melting behaviour of AOD and chromium converter slags. Steel research international. Vol. 75. 2004. No. 12. pp. 800-806.

II   Heikkinen, Eetu-Pekka, Riipi, Jaana & Fabritius, Timo. A computational study on the nitrogen content of liquid stainless steel in equilibrium with Ar-N$_2$-atmosphere. 7th International Conference on Clean Steel. 4-6. 6. 2007. Balatonfüred, Hungary. OMBKE & IOM. pp. 436-443.

III Riipi, Jaana, Fabritius, Timo, Heikkinen, Eetu-Pekka, Kupari, Pentti & Kärnä, Aki. Behavior of nitrogen during AOD process. ISIJ International. Vol. 49. 2009. No. 10. pp. 1468-1473.

IV Heikkinen, Eetu-Pekka, Fabritius, Timo & Riipi, Jaana. Holistic analysis on the concept of process metallurgy and its application on the modelling of the AOD process. Metallurgical and materials transactions B. Vol. 41B. 2010. No. 4. pp. 758-766.

V   Heikkinen, Eetu-Pekka, Ikäheimonen, Topi, Mattila, Olli & Fabritius, Timo. A thermodynamic study on the oxidation of silicon, carbon and chromium in the ferro-chrome converter. The twelwth international ferro alloy congress INFACON XII. 6-9.6.2010. Helsinki, Finland. pp. 229-237.

VI Heikkinen, Eetu-Pekka, Ikäheimonen, Topi, Mattila, Olli, Fabritius, Timo & Visuri, Ville-Valtteri. Behaviour of silicon, carbon and chromium in the ferrochrome converter - a comparison between CTD and process samples. The 6th European Oxygen Steelmaking Conference EOSC2011. 7-9.9.2011. Stockholm, Sweden. pp. 316-329.

Author's contribution on the original papers

I
Completely: Computational thermodynamics as well as discussion on its results.
Main part: Definition of the research topic, discussion on experimental results, writing.
Partly: Execution of the experiments.

II
Completely: Computational thermodynamics as well as discussion on its results, presentation in the conference.
Main part: Writing.
Partly: Definition of the research topic.

III
Completely: Computational thermodynamics as well as discussion on its results.
Partly: Definition of the research topic, non-thermodynamic modeling as well as discussion on its results, writing.

IV
Completely: Definition of the research topic, literature survey and evaluation, conceptual analysis, writing.
Main part: Evaluation of the conceptual analysis and its application on the modeling of the AOD process.

V
Completely: Definition of the research topic, computational thermodynamics as well as discussion on its results, presentation in the conference.
Main part: Comparison between computations and industrial samples, writing.
Partly: Industrial sampling.

VI
Completely: Definition of the research topic, computational thermodynamics as well as discussion on its results, presentation in the conference.
Main part: Comparison between computations and industrial samples, writing.
Partly: Industrial sampling.

List of abbreviations

AISI   American Iron and Steel Institute

AOD   Argon Oxygen Decarburization

BOF   Basic Oxygen Furnace

CAS-OB   Composition Adjustment by Sealed Argon Bubbling - Oxygen Blowing

CFD   Computational Fluid Dynamics

CRC   Ferrochrome Converter

CRE   Carbon Removal Efficiency

CTD   Computational Thermodynamics

EAF   Electric Arc Furnace

EDS   Energy Dispersive X-Ray Spectroscopy

IUPAC   International Union of Pure and Applied Chemistry

PBL   Problem-Based Learning

R&D   Research and Development

SAF   Submerged Arc Furnace

SEM   Scanning Electron Microscope

STP   Standard Temperature and Pressure according to IUPAC (273.15 K or 0 °C and 100 kPa or 1 bar, respectively)

VOD   Vacuum Oxygen Decarburization

XRF   X-Ray Fluorescence

List of symbols

A_{eff}	Effective surface area of a reaction
a_i, $a(i)$	Activity of component i
C	Concentration of considered element
C_e	Equilibrium concentration of the considered element
dy/dx	Derivative of 'y' with respect to 'x'
e	Base of the natural logarithm (approximately 2.71828)
f_i	Activity coefficient of component i
$\Delta G^0_{(i)}$	Standard Gibbs free energy for reaction presented in equation (i)
$\Delta G_{R \to H}$	Gibbs free energy for the change between Raoultian and Henrian standard states
[%i]	Content of component in wt-%
k_1	First-order rate constant
k_2	Second-order rate constant
$K_{(i)}$	Equilibrium constant for the reaction presented in equation (i)
m_i	Mass fraction of component i
p_i, $p(i)$	Partial pressure of component i
R	Gas constant (1.987 cal·mol^{-1}·K^{-1} = 8.314 J·mol^{-1}·K^{-1})
t	Time
T	Temperature
V	Volume
[wt-%]$_i$	(Equilibrium) Content of component i (in wt-%)
X_i, $X(i)$	Mole fraction of component i
α	Condition-specific constant in an equation describing the decarburization rate
β	Condition-specific constant in an equation describing the decarburization rate

20

Table of contents

22

1   Introduction

Although the annual production of stainless steels covers merely few percent of the global steel production, the significance of stainless steels is undeniable in certain applications. The most commonly used method in stainless steel production is Argon-Oxygen-Decarburization -process (AOD), in which the excessive oxidation of chromium is prevented by using argon to dilute the blowing gas during the final stages of the process (Krivsky 1973). In integrated steel plants in which stainless steel and ferrochrome are produced in a same location (such as in Outokumpu Tornio works), a so-called ferrochrome converter (CRC) can be used for pretreatment of ferrochrome before the AOD process.

In stainless steel production - and process engineering in general - it is essential to know the influence of process variables and conditions on the process outcome. In order to productionally, economically and ecologically optimize the refining processes (*e.g.* the previously mentioned AOD and CRC), one has to know these dependences between the process outcomes and variables. In an effort to obtain this knowledge, process modelling and simulation as well as experimental procedures and analyses can be used as valuable tools. (Heikkinen & Fabritius 2012). One of the key methods used in this work is computational thermodynamics (CTD), which helps us to consider, whether the chemical phenomena taking place in the processes are possible or not. In order to obtain more holistic view on these phenomena, one has to consider kinetics and mechanisms of chemical reactions, transport phenomena and material structures and properties as well. (Holappa & Taskinen 1983)

1.1   Context of research: Process metallurgy

The purpose of metallurgical research and development is to optimize metallurgical processes and products in a way that takes productional, economical, quality, ecological and safety aspects into account. This optimization requires information concerning the physical and chemical phenomena inside the processes. However, even a deep understanding of these phenomena is not sufficient alone without the knowledge concerning the connections between the phenomena and the applications. In order to understand these connections, metallurgical research and development should be considered from all the perspectives that are relevant in process metallurgy. This means that it is

necessary to consider the connections between theoretical and practical aspects of process metallurgy. (Heikkinen & Fabritius 2012)

Although the concept of metallurgy has been analysed in the literature (*e.g.* Bensaude-Vincent *et al.* 2004, Blicblau *et al.* 1994, Chipman 1949, Holappa & Taskinen 1983, Taskinen 2009), all these considerations fail to explicitly present the connections between the theoretical and practical aspects of metallurgy.

In Figure 1 the concept of process metallurgy is illustrated as an triangle with practice, research and education as its three aspects located in the corners. In Figure 1, research is considered to be connected with different scientific methodologies, whereas education is related to curricula. Practice is strongly linked with different kind of (industrial) applications. Link between research and education are the phenomena that are researched as well as taught/studied in order to understand the fundamentals of metallurgical processes. Connection between research and practice are individual cases and the link between education and practice are problem-based learning (PBL) and other educational methods in which actual problems and cases are integrated with pedagogical methods.

In order to avoid the previously mentioned shortcoming of previous considerations, it is necessary to find the connecting link between practice, research and education. Two things that are common to all three aspects are goals towards which the activity is directed and tools that are used to achieve these goals. Since the purpose of this thesis is to present the role of computational thermodynamics in metallurgical research and development, tools have been included in Figure 1 instead of goals.

To visualize the features of different aspects and to present the connections between these aspects more specifically, it is possible to make different kind of projections from Figure 1. While making these projections, one should keep in mind, that without taking the practical element into account one loses the applied nature of the engineering sciences and therefore all the projections should be drawn from the lower left-hand corner in which the practical applications are located.

Although it would be possible to consider the connections between practice and research as well as practice and education separately, it is more meaningful to create a projection from the practical corner to the side between research and education. With this kind of projection (presented in Figure 2) research and education are not separated as two distinct areas of academic activities. It is important to maintain the connection between these two in order to ensure the research-based education and to educate qualified research for the future.

24
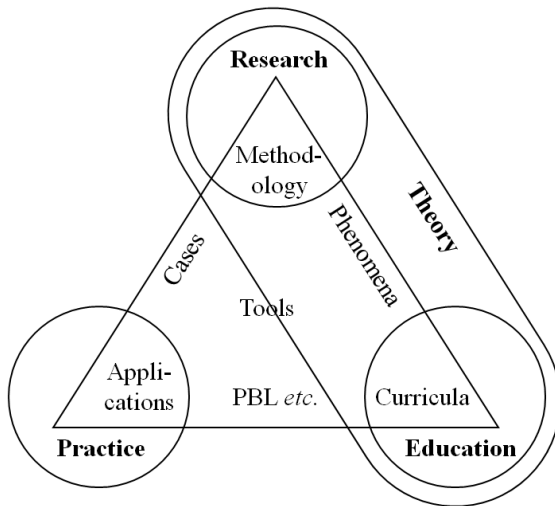
Fig. 1. Different aspects of process metallurgy and their characteristic features.
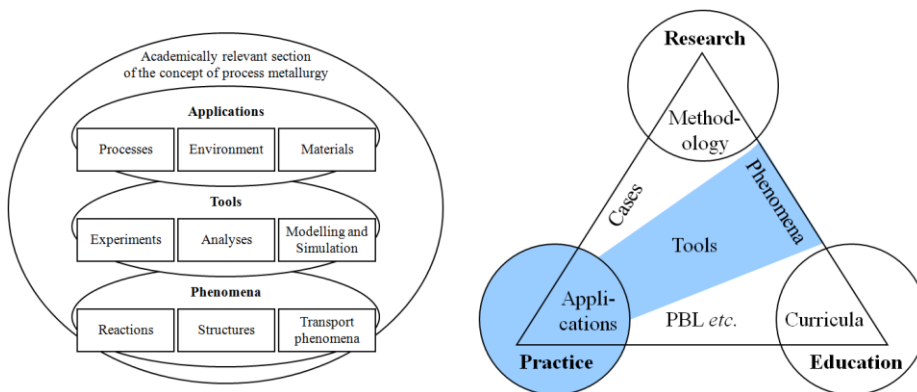
Fig. 2. Academically relevant projection of the concept of process metallurgy.

The top level in Figure 2 represents the applications which could be related to either processes (*i.e.* process development), environment (*i.e.* environmental and sustainability investigations) or materials (*i.e.* products, raw materials, refractory materials, residues, *etc.*). The bottom level illustrates the phenomena that are common to both research and education of process metallurgy. In metallurgical considerations the most significant phenomena are reactions (consideration of reaction mechanisms as well as thermodynamic and kinetic evaluations),

structures (*i.e.* their influence on properties as well as structural changes such as phase transitions) and transport phenomena (*i.e.* mass transfer, heat transfer and fluid dynamics). These phenomena are investigated and explained by experimental, analytical and modelling tools (middle level in Figure 2) that are used to apply the phenomenon-based considerations into practical applications. The role of the modelling - as well as other methods of research and development - as a connective link between the applications and phenomena is illustrated in more detail in Figure 3. It should be noted that due to sake of clarity Figure 1 does not contain all the applications, methods nor phenomena that could be related to the production of ferrochrome and stainless steels. Its purpose is to be merely an example of how the link between the applications and phenomena is created via modelling, analyses and experiments.
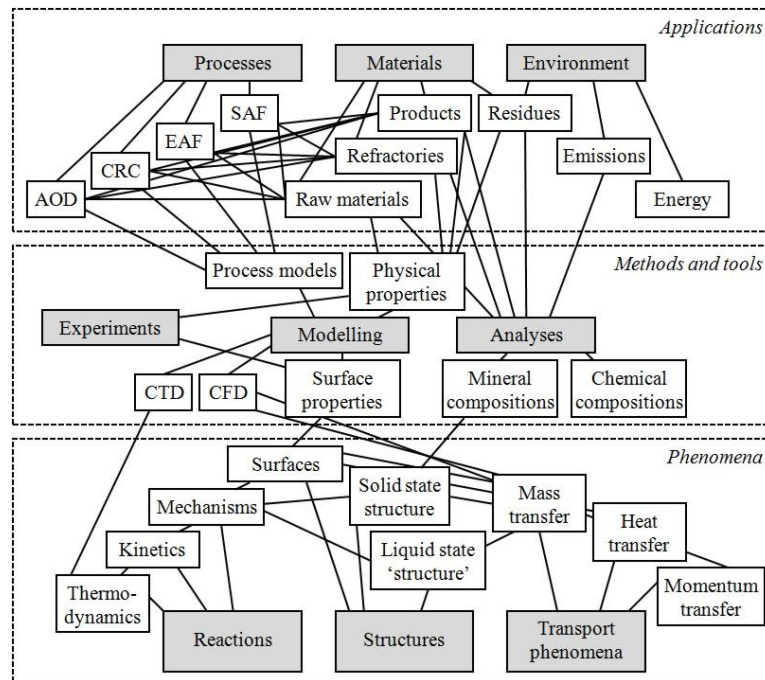
Fig. 3. Role of R&D methods as a connective link between the applications and the phenomena (Heikkinen & Fabritius 2012).

1.2 Goals of research

The goal of this thesis is to present the role of computational thermodynamics in metallurgical research and development of the stainless steelmaking refining processes. Using Figures 2 and 3 as a reference, this may be presented as a question on how computational thermodynamics is used to develop, optimize and understand the AOD and CRC processes by modelling the chemical reactions taking place in these processes - *i.e.* how computational thermodynamics may be used to connect metallurgical theory and practice in the context of stainless steelmaking.

As presented in Figure 3, the only direct connection of computational thermodynamics to the bottom level (*i.e.* phenomena), is to thermodynamics of chemical reactions. This, however, does not mean that computational thermodynamics would not be significant in consideration of other metallurgical phenomena as well. Primary condition for all the phenomena to occur is the existence of thermodynamic driving force, without which none of the phenomena can take place. Hence, computational thermodynamics, which can be used to estimate the driving forces of these phenomena, is an essential basis while considering any metallurgical phenomena or process (O'Connell 1993). Speed of reactions and kinetics of the reaction systems can be 'manipulated' by successful process design, but thermodynamic facts and rules we will always have to obey (Eketorp 1983).

To answer the question on how computational thermodynamics is used as a link between metallurgical theory and practice, it is necessary to consider:

1. What is the purpose of stainless steel refining processes and how are they operated?
2. What are the most relevant phenomena within these processes to be studied?
3. How these phenomena should be studied and what is the role of computational thermodynamics in these studies?

In this thesis, these questions are considered via three case studies, in which computational thermodynamics have been used in research and development of AOD and CRC processes. The case studies are chosen in a way that they represent (1) reactions between molten metal and molten slag, (2) reactions between molten metal and a gas phase as well as (3) reactions involving solid refractory materials in both CRC and AOD processes. The case studies are presented in Figure 4.

	Reactions between molten metal and slag	Reactions between molten metal and gas	Reactions involving refractory materials
CRC	Metal-slag equilibria concerning C, Si and Cr *Original papers V & VI*	Oxidation of C, Si and Cr	Melting and solidification of slags on refractory surface
AOD		Nitrogen pickup and removal *Original papers II & III*	Melting and solidification of slags on refractory surface *Original paper I*

Fig. 4. Three case studies in which computational thermodynamics were used in research and development of CRC and AOD processes.

The role of computational thermodynamics in understanding stainless steelmaking has been considered previously by Kho *et al.* (2010) and Swinbourne *et al.* (2010, 2012)[1], who used HSC Chemistry for Windows to study the chemical reactions in EAF, VOD and AOD processes[2]. Differing from their studies, this work focuses also on CRC process (in addition to AOD) and has a goal to explicitly present the role of computational thermodynamics as a link between metallurgical theory and practice (*cf.* Figures 2 and 3). Additionally, in this thesis the results of these considerations are also applied in pedagogical and curricular planning.

---

[1] Most of the studies in which computational thermodynamics are applied in the research and development of stainless steelmaking are focused on inclusions. However, these studies are not covered in this thesis, since inclusions are relevant in the unit operations succeeding the deoxidation and the focus of this thesis is on AOD and CRC processes; *i.e.* the operations preceding deoxidation.

[2] These considerations had certain limitations such as use of constant activity coefficients throughout the calculations (Swinbourne *et al.* 2012).

2 Processes

The process descriptions presented in this chapter are mainly based on the processes of the Outokumpu Stainless Tornio steel works, although some effort have been made to generalize the descriptions. The reason for choosing Tornio Works as an example is not only the fact that all the case studies presented in this thesis are based on Outokumpu's processes, but also because as an only integrated stainless steel plant in Europe (Riekkola-Vanhanen, 1999) it gives a comprehensive outlook on most of the unit operations that are relevant for stainless steelmaking. In fact, vacuum oxygen decarburization (VOD; *cf.* chapter 2.1.3 for more details) is the only significant process of stainless steelmaking that is not included in the Tornio works process route.

2.1 Stainless steel and its production

The purpose of this chapter is to give a short outlook on stainless steel and ferrochrome as well as their production in general. The two unit operations most relevant for this thesis, namely AOD and CRC processes, are presented in more detail in the following two chapters.

2.1.1 Stainless steel

The amount of stainless steel that is annually produced worldwide has increased from approximately 19 million metric tons in 2001 to approximately 33.5 million metric tons in 2010 (*Anon.* 2012a, *Anon.* 2012b). Although this is not much when compared to total annual production of crude steel (being approximately 1490 million metric tons in 2011; *Anon.* 2012c), there are certain areas of application in which the stainless steels have an essential role due to their resistance against corrosion (*e.g.* in construction, transport, process equipment, surgical instruments and catering appliances). Corrosion resistance is achieved by using chromium as an alloying element. In oxidizing conditions a thin yet dense layer is formed on the surface of the metal if the chromium content of the metal is over approximately 12 wt-% (*e.g.* Wranglén 1985). This layer passivates the metal and prevents corrosion in several corrosive media. (Heikkinen & Fabritius 2012, Kho *et al.* 2010, Swinbourne *et al.* 2010)

The amount of chromium in stainless steels typically varies from 12 wt-% to nearly 30 wt-%. In addition to chromium, stainless steels contain other alloying

elements that are used to adjust the structure as well as physical and chemical properties of the final product. The most commonly used grades of stainless steels are austenitic steels in which nickel is used as a third major component in addition to iron and chromium. Other major stainless steel grades are ferritic stainless steels (no nickel), martensitic stainless steels (less chromium in comparison to e.g. austenitic grades) and duplex steels (more chromium, some nickel). In addition to iron, chromium and nickel, some other elements are used in certain grades to enhance certain critical properties (e.g. molybdenum to enhance the corrosion resistance against acids) or to stabilize a certain structure (e.g. manganese to replace nickel as austenite stabilizer). Typical contents of main elements for different stainless steel grades are presented in Table 1. (Heikkinen & Fabritius 2012, Kho *et al.* 2010, Swinbourne *et al.* 2010)

Table 1. Typical compositions (in wt-%) of different kind of stainless steel grades (collected from various sources).

Grades	Cr	Ni	C	Si	Mn	Others	AISI grades
Austenitic	16-20	> 8	< 0.1	< 1	< 2	Mo, Nb, Ti	*e.g.* 304, 316, 317
Ferritic	11.5-17	-	< 0.1	< 1	< 1	Al, Ti	*e.g.* 405
Martensitic	11.5-17	- / < 2.5	0.1-0.4	< 1	< 1		*e.g.* 403, 410, 414
Duplex	> 22	4-6				Mo	
Cr-Mn austenitic	16-18	1-8	< 0.1	< 1	5-10		

2.1.2 Ferrochrome

All stainless steels contain chromium by definition. Hence, it is necessary either to alloy chromium or to use chromium-containing raw materials (*e.g.* ferrochrome and stainless steel scrap) in production of stainless steels. From economic point of view, the latter option is more suitable than the former. Of these raw materials, ferrochrome is usually produced from chromite ores and concentrates, in which both of the stainless steel's main components - *i.e.* iron and chromium - are present. Since the occurence and the availability of these raw materials is globally limited (Riekkola-Vanhanen 1999), the use of internal and/or recycled merchant stainless steel scrap as a raw material is essential in the production of stainless steels. For instance, in 2011 approximately 5 million metric tons of stainless steel

scrap were exported worldwide (*Anon.* 2012d) and it is estimated that the average content of recycled material in new stainless steel is over 60 % (*Anon.* 2012e). The end-of-life recycling rate of stainless steels is approximately 70 % (Reck *et al.* 2010). Typical compositions of ferrochrome as well as chromite ore and concentrates are presented in Table 2. The compositions of the stainless steel scrap correspond with the compositions presented already in Table 1. (Heikkinen & Fabritius 2012)

Table 2. Typical compositions (in wt-%) of ferrochrome as well as chromite ores and concentrates (collected from various sources).

	Cr	Fe	C	Si	O	Others
Ferrochrome	53-55	33-37	7	3-5	-	
Chromite ores and concentrates	25-31	12-19	-	1-6	32-37	Al: 4-15 Mg: 7-13

2.1.3 Stainless steel production

As mentioned in chapter 2.1.1, stainless steels are highly alloyed solutions of iron and chromium as well as other alloying elements that are used to obtain wanted chemical and mechanical properties for the final products. While producing these highly alloyed steels it is important to have processes in which the yields of valuable elements - such as chromium - are as high as possible. For refining processes in which elements such as carbon or silicon are being removed, this obviously sets certain challenges that are not encountered in the production of low-alloyed steels. Taking decarburization as an example, it is necessary not only to decrease the amount of carbon to a required level, but to prevent excessive oxidation of chromium at the same time. Due to this, some unit operations are usually executed using different kind of process solutions in low-alloyed steelmaking and stainless steelmaking, although there are certain similarities in the production routes as well. (Choulet *et al.* 1971, Heikkinen & Fabritius 2012, Kho *et al.* 2010, Swinbourne *et al.* 2010, Swinbourne *et al.* 2012, Wijk 1992)

One of the key issues in the production of stainless steels is to solve how to execute the above-mentioned decarburization without the simultaneous oxidation of chromium (Choulet *et al.* 1971, Swinbourne *et al.* 2010, Swinbourne *et al.* 2012, Wijk 1992); *i.e.* how to promote the oxidation reaction of carbon presented in Equation (1) and to prevent the oxidation reaction of chromium presented in Equation (2).

$$\underline{C}_{Fe} + \underline{O}_{Fe} = CO\ (g) \tag{1}$$

$$2\ \underline{Cr}_{Fe} + 3\ \underline{O}_{Fe} = (Cr_2O_3) \tag{2}$$

Use of basic oxygen furnace (BOF), which is widely used in the production of low-alloyed steels, would cause devastating oxidation of chromium, if it was used in the production of stainless steels. The oxidation reactions presented in equations (1) and (2) may be considered more precisely by studying the equilibrium constants (K) written for these reactions:

$$K_{(1)} = \frac{p_{CO}}{a_C \cdot a_O} = e^{-\frac{\Delta G^0_{(1)}}{R \cdot T}} \tag{3}$$

$$K_{(2)} = \frac{a_{Cr_2O_3}}{a_{Cr}^2 \cdot a_O^3} = e^{-\frac{\Delta G^0_{(2)}}{R \cdot T}} \tag{4}$$

in which p_i represents the partial pressure of component i, a_i represents the activity of component i, $\Delta G^0_{(x)}$ is standard Gibbs free energy for reaction (x) [in $J \cdot mol^{-1}$ or $cal \cdot mol^{-1}$], R is the gas constant [in $J \cdot mol^{-1} \cdot K^{-1}$ or $cal \cdot mol^{-1} \cdot K^{-1}$] and T is temperature [in K].

It is seen from equation (3) that to enhance the oxidation of carbon (at constant temperature) it is necessary to either increase the activity (and amount) of oxygen or to decrease the partial pressure of carbon monoxide in the system. According to equation (4) the increase in the activity of oxygen enhances also the oxidation of chromium and hence the only meaningful option is to decrease the partial pressure of CO. In order to do this, it is possible either to dilute the gas by blowing inert gases such as nitrogen and/or argon into the system or to decrease the total pressure of the system. The former method is used in AOD converters (Argon Oxygen Decarburization), whereas the latter is utilized in VOD converters (Vacuum Oxygen Decarburization). One of these converter types is used in nearly all stainless steel production routes. (Shimizu 2001, Swinbourne *et al.* 2010, Swinbourne *et al.* 2012, Wijk 1992) The AOD converters are more commonly used as approximately three quarters of the stainless steel world production is manufactured using an AOD. (Choulet & Masterson 1993, Hartenstein *et al.* 1997, Jones 2001, Swinbourne *et al.* 2012) On the other hand, the charge sizes of the VOD converters are usually smaller than the ones of the AOD, and therefore it is

often used in the steel works in which the annual production is smaller. (Heikkinen & Fabritius 2012)

Other unit operations of the stainless steel production are chosen based on the steel grades that are being produced as well as the raw materials that are being used. In scrap-based stainless steelmaking, electric arc furnace (EAF) is used to melt the scrap, after which the molten metal is further processed in AOD, VOD and/or various ladle treatments depending on the requirements set by the product. In other words melting and refining (*i.e.* mainly decarburization) are separated into two independent processes. If ferrochrome is used as a raw material, it is also melted in EAF unless the ferrochrome is produced in the same location, which enables the transfer of molten metal from the ferrochrome plant to the stainless steel plant. As for ferrochrome, it is most commonly produced in submerged arc furnaces (SAF) using chromite ores and/or concentrates as raw materials. A so-called ferrochrome converter (CRC) may be used as a pretreatment process between SAF and AOD, if ferrochrome is transfered to stainless steel plant in a molten state. (Heikkinen & Fabritius 2012, Kho *et al.* 2010, Swinbourne *et al.* 2010, Swinbourne *et al.* 2012, Wijk 1992)

The AOD (or VOD) is followed by ladle treatments, continuous casting, slab grinding, hot and cold rolling as well as pickling and annealing. Process flow sheet of the Outokumpu Stainless and Outokumpu Chrome Tornio Works is presented in Figure 5 as an example of the stainless steel production route.
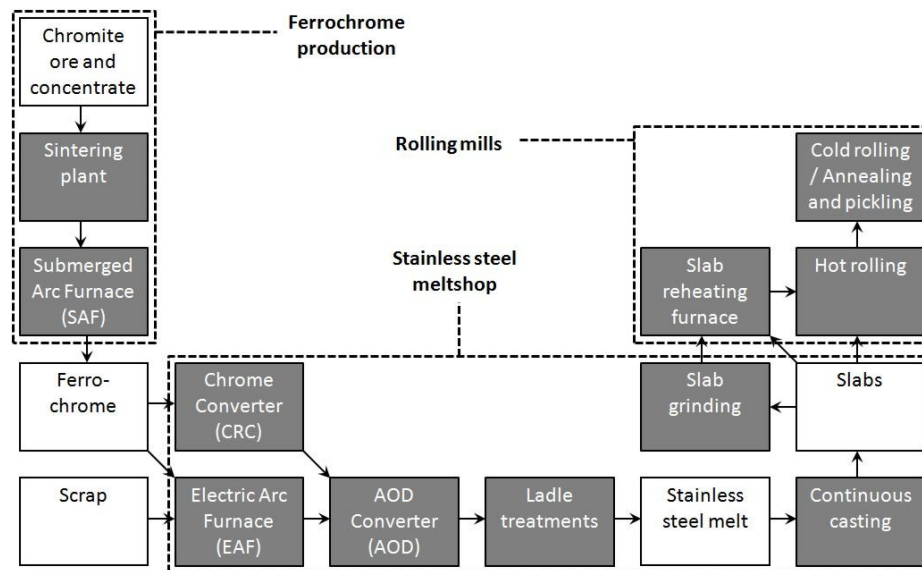
Fig. 5. Schematic presentation of the stainless steel production at the Outokumpu Chrome and Outokumpu Stainless Tornio Works (materials are presented in white boxes and processes in grey boxes).

2.2 AOD process

AOD converter (*cf.* Figure 6) is a process especially developed for stainless steelmaking. Its purpose is to remove carbon - as well as silicon if CRC is not being used - without excessive oxidation of chromium from the metal that consists of molten scrap and ferrochrome. Decarburization without excessive chromium oxidation is achieved by using argon to lower the partial pressure of carbon monoxide as explained in chapter 2.1.3. This allows higher chromium concentrations of the melt to be in equilibrium with lower carbon contents. Although the oxidation of chromium may be significantly lessened with argon, it is nevertheless necessary to have a reduction stage in which the oxidized chromium is reduced after the decarburization. (Fabritius 2004, Swinbourne *et al.* 2012, Wijk 1992)
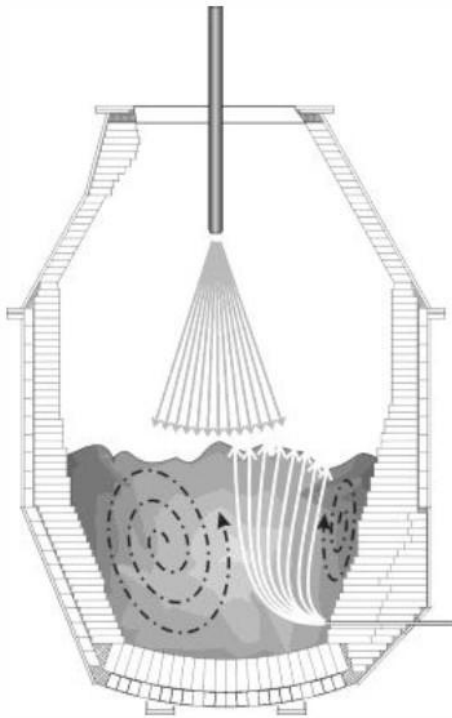
Fig. 6. Schematic presentation of an AOD converter. It should be noted that the ferrochrome converter is geometrically very similar to AOD presented in this figure. (Heikkinen & Fabritius 2012)

In addition to decarburization and reduction of chromium, other important features of the AOD process are nitrogen control and sulphur removal. To control the process it is important to know how to influence oxidation reactions and how to control the nitrogen content with accessible process variables. The variables with which the AOD is usually being optimized are the blowing ratios between top and bottom blowing, lance positions and oxygen/nitrogen/argon -ratios in the gas during the different stages of the blowing as well as the durations of stages themselves. Furthermore, it is possible to control the process via additions of scrap, lime and alloying elements. (Fabritius 2004, Swinbourne *et al.* 2012, Wijk 1992)

Refining of stainless steel in AOD process is divided into various stages based on the use of process variables mentioned above. During the first stages of refining, pure oxygen is blown into the steel melt via sidewall tuyeres and a top

lance in order to accelerate the removal of carbon and silicon. At these stages some chromium is also oxidised and transfered to the slag. As the decarburization proceeds, gas mixture is blown only through sidewall tuyeres. At the same time, the flow rate of oxygen is decreased and the flow rates of nitrogen and/or argon are increased in order to decrease the oxidation of chromium. The use of nitrogen increases the amount of soluble nitrogen in molten metal and must therefore be replaced by argon during the last stages of blowing. The stage following the decarburization is the combined desulphurization and slag reduction in which the oxidised chromium is reduced from the slag with silicon and during which only argon is blown into the melt. Silicon is added to the charge as ferrosilicon. CaF_2 is charged at the beginning of the slag reduction stage in order to lower the viscosity of the slag. Accurate slag basicity and fluidity are required in order to secure simultaneous sulphur removal and slag reduction. (Fabritius 2004, Swinbourne *et al.* 2012, Wijk 1992)

An example of different stages as well as carbon, chromium and nitrogen contents of the steel melt in the AOD process is presented in Figure 7 as a function of blowing time. Examples of typical compositions of the metal and slag phases are presented in Tables 3 and 4, respectively. (Fabritius 2004)

In Tornio stainless steel works there are two AOD converters. Nominal capacities of these converters are 95 and 150 metric tons. Dolomite is used as refractory material in both AOD converters.
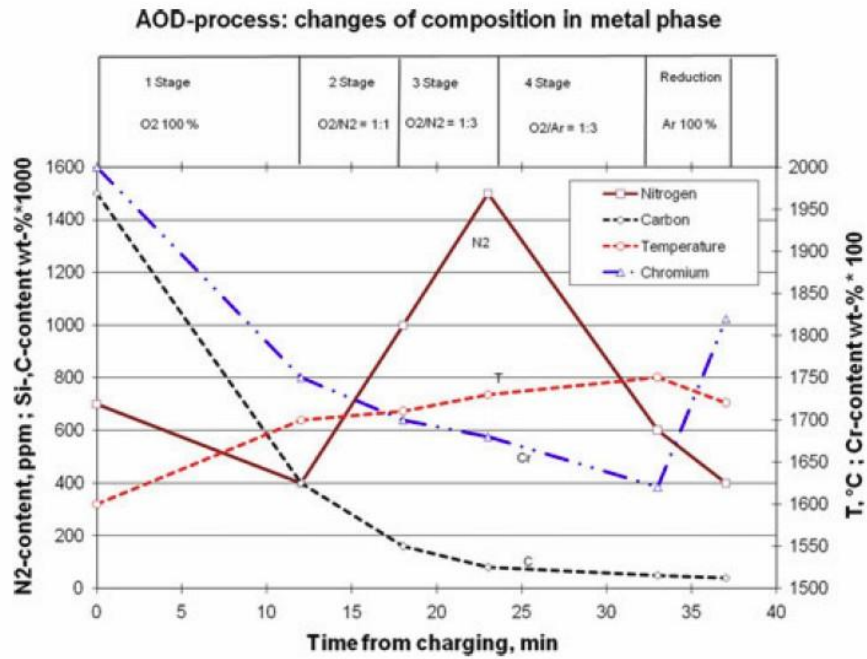
Fig. 7. An example of changes in metal composition during the AOD processing (Fabritius 2004, Kupari 2003).

Table 3. Typical metal compositions (in wt-%) and temperatures at the beginning and at the end of the AOD processing (Fabritius 2004).

	Cr	Ni	C	Si	Mn	S	T (°C)
Initial	20	6	2	0.1	0.7	0.025	1600
Finish	18	8	0.040	0.5	1.5	0.002	1680

Table 4. Typical slag composition (in wt-%) at the end of the AOD processing (Fabritius 2004).

CaO	SiO$_2$	MgO	Fe$_2$O$_3$	Cr$_2$O$_3$	Al$_2$O$_3$	TiO$_2$	CaF$_2$	Basicity
54-57	26-29	6.5-9	0.5-1	0.5-1.5	1-2	0.3-1	7-10	1.9-2.2

2.3 CRC process

In comparison to AOD process, which is widely used in the production of stainless steels, the use of ferrochrome converter (CRC) is much more limited. Due to its role as a link between the productions of ferrochrome and stainless steels, its utilisation is mainly limited to the plants, in which both ferrochrome and stainless steel are produced in the same location. CRC process may be considered as a link between ferrochrome and stainless steel productions, because its product is a raw material for AOD, whereas its raw materials are molten ferrochrome with high silicon and carbon contents (from the ferrochrome plant) and stainless steel scrap that is used to decrease the melt's temperature that is increased due to oxidation reactions of silicon and carbon.

The purpose of the CRC process is to serve as a buffer for liquid ferrochrome, to remove silicon and some carbon from ferrochrome and to use the released heat for scrap melting. The geometries of CRC and AOD converters are very similar (both having sidewall tuyeres in addition to top lance and almost identical shapes; *cf.* Figure 6 in chapter 2.2) and this similarity enables the use of CRC as an AOD in case of an AOD breakdown. (Fabritius 2004) Despite the geometrical similarities, the refractory materials used in CRC differ from the ones used in the AOD. Whereas the AOD has dolomitic linings, magnesia-carbon-bricks are used as refractory materials in the CRC.

During the CRC process oxygen is blown into the metal, due to which the silicon content of the metal is decreased from 4 to 5 wt-% to less than 0.5 wt-%. At the same time, the carbon content is decreased from approximately 7 wt-% to approximately 3 wt-%. Further decarburization would lead into excessive oxidation of chromium. Exothermic oxidation reactions of silicon and carbon release energy that is used to heat the metal and to melt scrap and slag formers. During the CRC process, 550 kg of scrap and 150 kg of slag formers per ton of produced ferrochromium are melted. (Fabritius 2004, Fabritius & Kupari 1999, Fabritius *et al.* 2001a, Fabritius *et al.* 2001b, Virtanen *et al.* 2004) The process variables that may be used to optimize and to control the CRC process are similar to the ones of the AOD process: proportions of oxygen, nitrogen and argon in the blowing gases, the amounts of gases blown through the lance and the tuyeres, lance height, durations of different blowing stages as well as lime and scrap additions (Heikkinen & Fabritius 2012).

Different stages of the CRC process as well as oxidation of silicon, carbon and chromium are illustrated in Figure 8 in which the Cr_2O_3-content of the slag as

well as the Si- and C-contents of the metal are shown as a function of the amount of blown oxygen (Fabritius 2004, Larkimo 1996). In the beginning approximately 60 m^3/min (STP) of oxygen is blown through the tuyeres (*cf.* stage 6 in Figure 8). This stage is followed by stage 22 (*cf.* Figure 8) during which approximately 50 m^3/min (STP) of air is blown through the tuyeres in addition to approximately 130 m^3/min (STP) of oxygen that is blown through top lance. The final stage is similar to the first stage with the oxygen blowing of approximately 60 m^3/min (STP) through the tuyeres. The processing time is approximately 40-50 minutes depending on the charge weight. In Outokumpu Stainless Tornio works there is one CRC converter with a nominal capacity of 95 tons. Normally the charge weight varies from 30 to 100 tons. (Fabritius 2004)

Typical compositions of the metal and slag phases in the CRC process are presented in Tables 5 and 6, respectively.
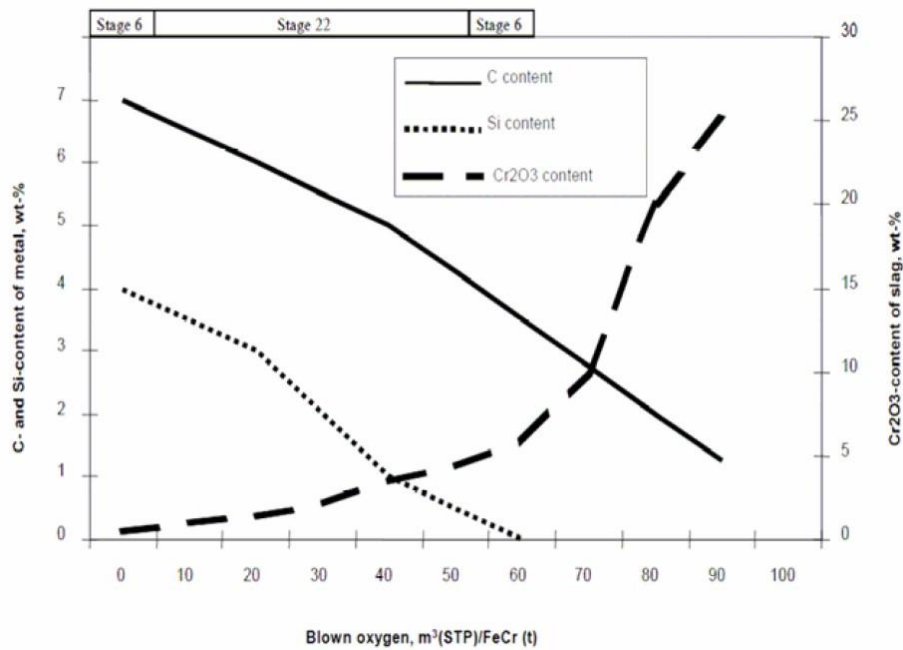
Fig. 8. Changes of slag and metal compositions during the CRC processing (Fabritius 2004, Larkimo 1996).

Table 5. Typical metal compositions (in wt-%) and temperatures during the CRC processing (partly from Fabritius 2004).

	Cr	Ni	C	Si	Mn	T (°C)
Initial	49-54	0.2	5.5-7	3-5	0.3	1520-1530
Intermediate	49-54		4-5	1		
Finish	35-39	0-5	2.5-3.5	0.1-0.4	0.4	1560-1700

Table 6. Typical slag composition (in wt-%) at the end of the CRC processing (Fabritius 2004).

CaO	SiO_2	MgO	Fe_2O_3	Cr_2O_3	Al_2O_3	TiO_2	CaF_2	Basicity
36-45	30-38	9-20	0.5-2	2-3	2-3.5	1-2	0.5-1	1.2-2

3 Phenomena

Metallurgically relevant phenomena may be divided into three categories: chemical reactions, transport phenomena and structural changes (as presented in Figures 2 and 3 in chapter 1.1). Since the purpose of this thesis is to focus on the role of computational thermodynamics in metallurgical R&D, the emphasis of this chapter is mainly on chemical reactions and less on transport phenomena and structural changes. However, in order to give a more comprehensive outlook on the phenomena taking place in AOD and CRC processes, transport phenomena and structrural changes are also briefly covered in chapters 3.2 and 3.3, respectively.

3.1 Chemical reactions

The most important chemical reactions in both AOD and CRC processes are carbon and silicon removal by oxidation (desired reactions) as well as oxidation of chromium (undesired reaction) (*e.g.* Swinbourne *et al.* 2012, Wijk 1992). In addition to these reactions, a few important reactions are characteristic only to the reduction stage of the AOD process: chromium oxide is being reduced back to the metal (*e.g.* Swinbourne *et al.* 2012, Wijk 1992), whereas sulphur is being removed from the metal into the slag (*e.g.* Wijk 1992). Absorption and desorption of nitrogen also involve a chemical reaction, since dissolution of nitrogen from gas into the metal features a decomposition of N_2 molecules into nitrogen atoms (*e.g.* Battle & Pehlke 1986, Lee & Morita 2003, Ono-Nakazato *et al.* 2003). Similarly, dissolution of lime into the slag features a decomposition of CaO into Ca^{2+} and O^{2-} -ions (*e.g.* Turkdogan 1996) and hence includes a chemical reaction. Finally, interactions between molten metal, slag and refractory materials involve chemical reactions, which may lead into a dissolution of the lining materials or into a formation of new phases on the interface (*e.g.* Janke & Ma 1999).

The most important reactions in AOD and CRC processes are collected in Table 7, in which the reactions are divided in three categories: (1) reactions involving only liquid phases, (2) reactions between a liquid and a gas phase and (3) reactions involving solid phases.

Table 7. The most important chemical reaction taking place in AOD and CRC processes.

	Reactions involving only liquid phases	Reactions between a liquid and a gas phase	Reactions involving solid phases
AOD	$\underline{Cr}$-(Cr_2O_3) -equilibrium (incl. reduction of Cr) $\underline{Si}$-(SiO_2) -equilibrium Sulphur removal Deoxidation with silicon	Oxidation and removal of Si Oxidation and removal of C Oxidation of chromium **Nitrogen absorption/desorption**	Dissolution of lime **Reactions involving refractory materials**
CRC	**$\underline{Cr}$-(Cr_2O_3) -equilibrium** **$\underline{Si}$-(SiO_2) -equilibrium**	**Oxidation and removal of Si** **Oxidation and removal of C** **Oxidation of chromium**	Dissolution of lime **Reactions involving refractory materials**

Reactions written in bold in Table 7 were chosen as case studies and they are presented in more detail in chapters 3.1.1 - 3.1.3. These phenomena have also been studied in five original papers (I, II, III, V and VI) that are presented as supplements of this thesis.

3.1.1 Liquid-gas -reactions

Oxidation of silicon, carbon and chromium

In chapter 2.1.3 the oxidation reactions of carbon and chromium were presented as reactions in which dissolved elements reacted with each other:

$$\underline{C}_{Fe} + \underline{O}_{Fe} = CO \text{ (g)} \tag{1}$$
$$2\ \underline{Cr}_{Fe} + 3\ \underline{O}_{Fe} = (Cr_2O_3) \tag{2}$$

In reactions presented in equations (1) and (2) it is assumed that the blown oxygen is first dissolved into metal, after which the dissolved oxygen reacts with either dissolved carbon or chromium. This assumption is reasonable, when considering oxidation reactions inside the metal bath, *e.g.* at the bubble-metal-interfaces. In the jet impact region a direct oxidation via gaseous oxygen is also possible. (Deo & Boom 1993) Direct oxidation reactions for silicon, carbon and chromium are presented in equations (5) to (8). Individual reactions (5) and (6) are used to describe the oxidation of silicon and carbon, respectively, whereas the

oxidation of chromium is described with two separate reactions (7) and (8) the previous describing the formation of chromium(III)oxide (Cr_2O_3) and and the latter the formation of chromium(II)oxide (CrO). The equilibrium constants for the reactions (5) to (8) are presented in equations (9) to (12), respectively.

$$\underline{Si}_{Fe} + O_2 \text{ (g)} = (SiO_2) \tag{5}$$
$$2 \underline{C}_{Fe} + O_2 \text{ (g)} = 2 CO \text{ (g)} \tag{6}$$
$$4/3 \underline{Cr}_{Fe} + O_2 \text{ (g)} = 2/3 (Cr_2O_3) \tag{7}$$
$$2 \underline{Cr}_{Fe} + O_2 \text{ (g)} = 2 (CrO) \tag{8}$$
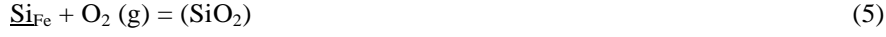
$$K_{(5)} = \frac{a_{SiO_2}}{a_{Si} \cdot p_{O_2}} = \frac{a_{SiO_2}}{f_{Si} \cdot X_{Si} \cdot p_{O_2}} = e^{-\left(\frac{\Delta G^0_{(5)} + \Delta G_{R \to H}}{R \cdot T}\right)} \tag{9}$$

$$K_{(6)} = \frac{p^2_{CO}}{a^2_C \cdot p_{O_2}} = \frac{p^2_{CO}}{f^2_C \cdot X^2_C \cdot p_{O_2}} = e^{-\left(\frac{\Delta G^0_{(6)} + \Delta G_{R \to H}}{R \cdot T}\right)} \tag{10}$$

$$K_{(7)} = \frac{a^{2/3}_{Cr_2O_3}}{a^{4/3}_{Cr} \cdot p_{O_2}} = \frac{a^{2/3}_{Cr_2O_3}}{f^{4/3}_{Cr} \cdot X^{4/3}_{Cr} \cdot p_{O_2}} = e^{-\left(\frac{\Delta G^0_{(7)} + \Delta G_{R \to H}}{R \cdot T}\right)} \tag{11}$$

$$K_{(8)} = \frac{a^2_{CrO}}{a^2_{Cr} \cdot p_{O_2}} = \frac{a^2_{CrO}}{f^2_{Cr} \cdot X^2_{Cr} \cdot p_{O_2}} = e^{-\left(\frac{\Delta G^0_{(8)} + \Delta G_{R \to H}}{R \cdot T}\right)} \tag{12}$$

in which a_i represents the activity of component i, p_i the partial pressure of component i, X_i the mole fraction of component i and f_i the activity coefficient of component i. $\Delta G^0_{(n)}$ equals the standard Gibbs energy for the reaction presented in Equation (n), $\Delta G_{R \to H}$ equals the Gibbs energy for the change between the Raoultian and Henrian standard states, R equals the gas constant (1,987 cal·mol^{-1}·K^{-1} = 8,314 J·mol^{-1}·K^{-1}) and T equals temperature.

Nitrogen absorption and desorption

One of the differences between the AOD and CRC processes concerns the behaviour of nitrogen. Whereas the CRC process is a pretreatment unit for the stainless steel production, in which the control of nitrogen is not yet essential, it is

important to control the amount of nitrogen of the metal during the AOD process in order to be able to produce stainless steel grades with strict composition limits. In the early stages of the AOD process the blowing gas consists of pure oxygen, but in order to decrease the oxidation of chromium - and to be able to reduce Cr_2O_3 during the reduction stage - the oxygen needs to replaced by nitrogen and argon. The use of cheaper nitrogen can be justified with economic reasons in the earlier stages, but due to nitrogen pick-up (of up to 1000 ppm) it is necessary to use more expensive argon during the last stage of decarburisation and the reduction stage. In order to control the nitrogen content of the metal, it is necessary to know the mechanisms of nitrogen absorption and desorption as well as the effect of process variables on the nitrogen pick-up (during the stages in which nitrogen is blown into the system) and nitrogen removal (during the stages in which argon is used). (*e.g.* Heikkinen & Fabritius 2012, Kärnä *et al.* 2008)

Absorption and desorption of nitrogen between gas phase and molten metal may occur by either single-site or dual-site mechanism. Desorption by single-site mechanism and absorption by dual-site mechanism are presented schematically in Figures 9 and 10, respectively. In desorption by single-site mechanism (*cf.* Figure 9) dissolved nitrogen atom is transferred to the interface, in which it meets another nitrogen atom and these two react to form a nitrogen molecule, N_2. Nitrogen molecule is then transferred into the gas phase by diffusion and convection. In absorption by dual-site mechanism (*cf.* Figure 10) nitrogen molecule is transferred from the gas phase to the gas/melt -interface, where it dissociates into two nitrogen atoms that are transferred into the bulk melt. The single-site mechanism is the only possible mechanism if the contents of surface active elements (such as oxygen and sulphur) are high, because these elements have a tendency to block the movement of adsorbed nitrogen atoms on the surface. On the other hand, the dual-site mechanism is more probable, if the contents of surface active elements are low. (Battle & Pehlke 1986, Lee & Morita 2003, Ono-Nakazato *et al.* 2003)
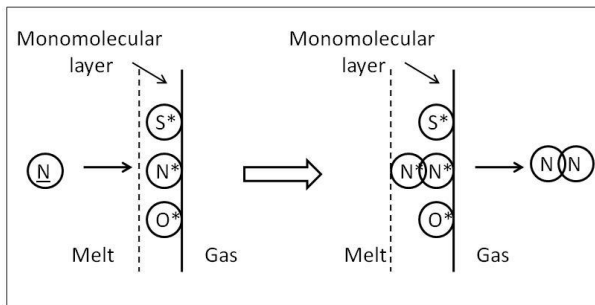
Fig. 9. Desorption of nitrogen by single-site mechanism.
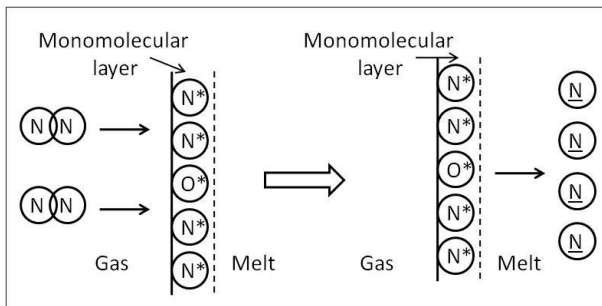
Fig. 10. Absorption of nitrogen by dual-site mechanism.

When considering the nitrogen absorption and desorption in the AOD process, it is reasonable to assume, that nitrogen transfer follows dual site mechanism during the first stages and single site mechanism during the last stages of the AOD process. This is based on the changes in the composition of the blowing gas and in the contents of carbon and silicon of the stainless steel melt during the blowing. During the first stages of decarburization the content of dissolved oxygen is very low due to high silicon and carbon contents. During the later stages the amount of dissolved oxygen in the metal begins to increase due to decreased amounts of carbon and silicon.

3.1.2 Reactions involving only liquid phases

Correlations between the amounts of chromium, silicon and carbon in molten metal and slag may be studied by defining the chemical equilibria for the slag-metal-reactions presented in equations (13) to (15) (*e.g.* Swinbourne *et al.* 2012).

The equilibrium constants for the reactions presented in Equations (13) to (15) are presented in Equations (16) to (18), respectively.

$$3\ \underline{Si}_{Fe} + 2\ (Cr_2O_3) = 3\ (SiO_2) + 4\ \underline{Cr}_{Fe} \tag{13}$$

$$2\ \underline{C}_{Fe} + (SiO_2) = 2\ CO\ (g) + \underline{Si}_{Fe} \tag{14}$$

$$3\ \underline{C}_{Fe} + (Cr_2O_3) = 3\ CO\ (g) + 2\ \underline{Cr}_{Fe} \tag{15}$$

$$K_{(13)} = \frac{a_{SiO_2}^3 \cdot a_{Cr}^4}{a_{Si}^3 \cdot a_{Cr_2O_3}^2} = \frac{a_{SiO_2}^3 \cdot f_{Cr}^4 \cdot X_{Cr}^4}{f_{Si}^3 \cdot X_{Si}^3 \cdot a_{Cr_2O_3}^2} = e^{-\left(\frac{\Delta G_{(13)}^0 + \Delta G_{R \rightarrow H}}{R \cdot T}\right)} \tag{16}$$

$$K_{(14)} = \frac{p_{CO}^2 \cdot a_{Si}}{a_C^2 \cdot a_{SiO_2}} = \frac{p_{CO}^2 \cdot f_{Si} \cdot X_{Si}}{f_C^2 \cdot X_C^2 \cdot a_{SiO_2}} = e^{-\left(\frac{\Delta G_{(14)}^0 + \Delta G_{R \rightarrow H}}{R \cdot T}\right)} \tag{17}$$

$$K_{(15)} = \frac{p_{CO}^3 \cdot a_{Cr}^2}{a_C^3 \cdot a_{Cr_2O_3}} = \frac{p_{CO}^3 \cdot f_{Cr}^2 \cdot X_{Cr}^2}{f_C^3 \cdot X_C^3 \cdot a_{Cr_2O_3}} = e^{-\left(\frac{\Delta G_{(15)}^0 + \Delta G_{R \rightarrow H}}{R \cdot T}\right)} \tag{18}$$

in which a_i represents the activity of component i, p_i the partial pressure of component i, X_i the mole fraction of component i and f_i the activity coefficient of component i. $\Delta G^0_{(n)}$ equals the standard Gibbs energy for the reaction presented in Equation (n), $\Delta G_{R \rightarrow H}$ equals the Gibbs energy for the change between the Raoultian and Henrian standard states, R equals the gas constant and T equals temperature.

3.1.3 Reactions involving solid phases

Refractory materials used in the AOD and CRC converters should obviously react with molten slag and metal as little as possible, since increased reaction rates lead into increased wear of the lining and may also cause problems with the process due to changed slag and steel compositions. Despite the efforts of having lining materials that are chemically, thermally and mechanically as stable as possible, reactions between the refractory material and molten phases do occur in the AOD and CRC processes. For example high and fluctuating temperatures, turbulent flow conditions, changes from oxidizing to reducing conditions as well as changes in the basicity of the slag are factors that increase the reactions between

dolomitic refractory materials and molten phases in the AOD converter. (Hartenstein *et al.* 1997, Shimizu 2001, Tikkanen *et al.* 1984)

To obtain longer campaign times for the AOD and CRC linings, it is necessary either to reduce the wear of the refractories in certain critical areas (*i.e.* tuyere zone in CRC and tuyere zone and trunnion area in AOD) or to protect these areas during the campaigns (Fabritius *et al.* 2000, Fabritius *et al.* 2001a). One way to prolong the campaign lifes is slag protection, in which converter slag is left to solidify on the critical areas of the converter walls after the tapping of the steel. In basic oxygen furnaces it is a commonly used practice to use so-called slag splashing, in which slag is splashed with a nitrogen pulse to the furnace walls (*e.g.* Ghosh *et al.* 2002, Krauss *et al.* 2004, Messina 1996, Peaslee 1996). In AOD and CRC converters the slag protection has been executed by tilting; *i.e.* molten slag is spread to the walls by swaying the converters back and forth.

Since the properties of the slag as well as interactions between slag and refractory have a strong effect on the success of the slag protection (Krauss *et al.* 2004, Madías *et al.* 2001), it is important to know the melting and solidification behaviour of the AOD and CRC slags in order to be able to estimate the chemical and mechanical stabilities of the solidified phases. One of the key issues in the slag protection of the AOD and CRC linings is to avoid the formation of di-calcium silicate during the solidification of the slag. If di-calcium silicate is formed, its phase transformation from β-form to γ-form during the cooling will disintegrate the material due to an 11% volumetric change accompanied with this phase transformation. (Deer *et al.* 1986, Eriksson & Björkman 2004).

3.2 Transport phenomena

To have a more comprehensive outlook on the AOD and CRC processes, it is necessary to study the non-chemical phenomena of the processes as well. One of the key issues is to understand the influence of blowing parameters on the flowing patterns of the liquid metal. This is important not only due to flow pattern's influence on the reactions, but also due to optimization of sufficient mixing and minimisation of unwanted spitting and splashing. (Heikkinen & Fabritius 2012) Since the focus of this thesis is on computational thermodynamics, only a brief summary on the studies concerning the fluid dynamics in AOD and CRC processes is given here.

The flow patterns may be studied by using either physical or numerical models; *i.e.* water-models and computational fluid dynamics (CFD), respectively.

Successful use of computational fluid dynamics to model extremely turbulent conditions inside the converters requires very fine computational grids as well as ability to express all the relevant phenomena mathematically[3]. This makes it often easier to use physical water models to investigate the flow patterns of the converters[4]. By constructing physical models with dynamic similarities to real processes, it is not necessary to know mathematical expressions for all the interdependencies between the process parameters and variables as long as it is possible to ensure the dynamic similarities between the model and the real process. Confirmation of these similarities is defined by using dimensioless numbers such as Froude's, Reynold's, Weber's, Ohnesorge's and Morton's numbers which describe the ratios between different forces in the model and in the real process. The values of a certain dimensioless number defined for the model and for the real process should be set as close to equal as possible by choosing the model geometry in a way that corresponds with the real process. (*e.g.* Fabritius & Kupari 1999, Fabritius *et al.* 2001a, Fabritius *et al.* 2001b, Heikkinen & Fabritius 2012, Virtanen et al. 2004)

Flow patterns of the AOD and CRC converters of the Outokumpu Stainless Tornio works have been studied using physical water models in several previous studies, in which the industrial data from Tornio has been used to validate the results of the modelling. The results of these studies indicate that the rates of the oxidation reactions of silicon and carbon may be increased due to enhanced mixing by increasing the total amount of gas blowing and by increasing the amount of inert gas that is blown through the sidewall tuyeres. These changes have also been noticed to increase the penetration of the tuyere gas jets and hence decrease the occurrence of the so-called back-attack phenomenon that is detrimental to the refractory materials close to the tuyeres. Another results from the flow pattern studies suggest that the removal of silicon can be improved by using a higher lance position at the first stage of the blowing, whereas the

---

[3] The key issues to be considered in the CFD modelling of the AOD are model geometry, grid distribution, behaviour of free surface, introduction and removal of materials into the system, modelling of turbulence and the interaction between different phases. Additionally, one has to consider whether it is necessary to take heat transfer and chemical reactions into account. It is usually easier and faster to consider isothermal and non-reactive systems, although in some cases this might lead into oversimplification of the model. (Gittler *et al.* 2000, Tang *et al.* 2004, Tilliander *et al.* 2004)

[4] As the name suggests, water is used in physical water models to illustrate the metal due to kinematic similarities between the liquid water at room temperature and liquid steel at approximately 1600 °C. On the other hand, its transparency helps to make observations inside the process.

removal of carbon in the later stages is improved with a lower lance position. The oxidation of chromium has been observed to decrease with the use of a top lance with wider nozzle angles. Furthermore, the physical models have been used to illustrate how the change from one-hole lance to three-hole lance in CRC process decreases unwanted spitting and splashing in the converter and hence enables the use of greater gas volumes - and increased productivity - without increasing the amount of metal losses due to splashing. In AOD the main circular flow has been observed to change its direction depending on the ratio between bath height and diameter as well as on the intensity of the gas blowing through sidewall tuyeres. Finally, the melt oscillation inside the AOD converter has been observed to depend on sidewall blowing and it is most likely to occur during the end of the decarburisation stage or during the reduction stage if tuyeres with large diameters are being used. With smaller tuyeres the penetration of the gas jets is deeper and the oscillation occurs most likely during the decarburisation stage. (Fabritius & Kupari, 1999, Fabritius *et al.* 2000, Fabritius *et al.* 2001a, Fabritius *et al.* 2001b, Fabritius *et al.* 2003, Fabritius *et al.* 2005, Virtanen *et al.* 2004)

3.3   Changes in material structures

Structural changes relevant for AOD and CRC processes are related to either melting and solification of materials or solid-state phase transformations within the materials. These phenomena include melting and dissolution of raw materials (*i.e.* scrap, lime, doloma, *etc.*), formation of liquid phases in the reactions between refractory materials and molten phases (*i.e.* slag and metal), solid-state phase transformations within the refractory material due to its reactions with molten phases and solidification of solid phases within the slag due to exceeded solubilities. (*e.g.* Shimizu 2001, Swinbourne *et al.* 2012, Tikkanen *et al.* 1984, Wijk 1992)

Structural changes considered in the case studies of this thesis were related to the solidification and melting behaviour of AOD and CRC slags as well as possibilites to use these slags to protect the converter linings as presented already in chapter 3.1.3.

4 Methods

Methods used in metallurgical research and development may be divided into three categories: models, analyses and experiments (as presented in Figures 2 and 3 in chapter 1.1). The target of the modelling may be either processes (*i.e.* process modelling) or material properties and phenomena (*i.e.* phenomenon-based modelling). The phenomenon-based modelling may be further divided into analytical, numerical and physical modelling. Analytical models consist of equations describing the effect of certain variables on the modelled property in a way that is solvable analytically. In numerical models these interdependencies between the properties and certain variables are solved using numerical optimization/minimisation methods. Typical examples of numerical modelling are computational fluid dynamics (CFD) and computational thermodynamics (CTD). In addition to these computational models, some models are based on physical analogies between a real system and a physical model. An example of this kind of physical modelling is the modelling of metal and/or slag flows using small scale water models (*cf.* chapter 3.2). (Heikkinen & Fabritius 2012)

Essential features that needs to be considered in the modelling of the phenomena taking place in the AOD and CRC converters are presented in Table 8.

Table 8. Essential features in the modelling of the phenomena taking place in the AOD and CRC processes (Heikkinen & Fabritius 2012).

	Main purpose of the process	Key issues to be modelled	Influencing factors	Variables needed to be cosidered in the modelling
AOD	Decarburization	Decarburization Control of N-pickup Prevention of oxidation of Cr Sulphur removal	Oxidation and reduction reactions (metal, slag) Interfacial properties Convection Viscosities	Blowing practice (durations of stages; proportions of O_2, N_2 and Ar; lance height; top/bottom blowing) Lime and scrap additions
CRC	Silicon removal	Removal of Si (and partly C) from metal Prevention of oxidation of Cr	Oxidation and reduction reactions (metal, slag) Interfacial properties Convection Viscosities	Blowing practice (durations of stages; proportions of O_2, N_2 and Ar; lance height; top/bottom blowing) Lime and scrap additions

Since the purpose of this thesis is to focus on computational thermodynamics, experiments and analyses as well as non-thermodynamic modelling are considered in this chapter only as tools to validate the results of thermodynamic modelling, although the validation is obviously not the only way to utilize these methods.

4.1 Modelling of chemical reactions

Chemical reactions may be considered thermodynamically (*i.e.* definition of chemical equilibria) and kinetically (*i.e.* definition of reaction rates). Thermodynamics focus on initial and final stages of considered systems, whereas in kinetic considerations it is necessary to be familiar with the reaction mechanisms.

While modelling the reactions in the AOD and CRC processes it is essential to consider how the oxidation reactions of silicon, carbon and chromium (i.e. removal of silicon and carbon as well as prevention of chromium oxidation) are influenced by process variables such as metal and slag compositions as well blowing rates. Knowledge concerning the interdependencies between the oxidation reactions and process variables enables the optimization of process parameters such as blowing practices and lime and scrap additions.

Although the focus of this chapter is on computational thermodynamics, the reaction kinetics concerning decarburization as well as absorption and desorption of nitrogen are also briefly covered.

4.1.1 Computational thermodynamics

Liquid-gas -reactions: Oxidation of silicon, carbon and chromium

Spontaneities of oxidation of silicon, carbon and chromium at different stages of the CRC process were estimated with thermodynamic computations validated with process samples from the Outokumpu Stainless Tornio works.

Thermodynamic equilibria for the oxidation reactions presented in equations (5) to (8) were compared with each other by using the partial pressures of oxygen (p_{O2}) characteristic for each reaction as parameters describing the equilibria. Smaller value of p_{O2} for a certain oxidation reaction indicates that less oxygen is

needed for oxidation when compared to a reaction for which the value of p_{O2} is larger. Partial pressures of oxygen corresponding the equilibrium between silicon and SiO_2, carbon and CO, chromium and Cr_2O_3 as well as chromium and CrO were calculated using equations (19) to (22), that were derived from the equations (9) to (12), respectively.

$$p_{O_2} = \frac{a_{SiO_2}}{f_{Si} \cdot X_{Si}} \cdot e^{\left(\frac{\Delta G^0_{(5)} + \Delta G_{R \to H}}{R \cdot T} \right)}$$

(19)

$$p_{O_2} = \frac{p^2_{CO}}{f^2_C \cdot X^2_C} \cdot e^{\left(\frac{\Delta G^0_{(6)} + \Delta G_{R \to H}}{R \cdot T} \right)}$$

(20)

$$p_{O_2} = \frac{a^{2/3}_{Cr_2O_3}}{f^{4/3}_{Cr} \cdot X^{4/3}_{Cr}} \cdot e^{\left(\frac{\Delta G^0_{(7)} + \Delta G_{R \to H}}{R \cdot T} \right)}$$

(21)

$$p_{O_2} = \frac{a^2_{CrO}}{f^2_{Cr} \cdot X^2_{Cr}} \cdot e^{\left(\frac{\Delta G^0_{(8)} + \Delta G_{R \to H}}{R \cdot T} \right)}$$

(22)

in which a_i represents the activity of component i, p_i the partial pressure of component i, X_i the mole fraction of component i and f_i the activity coefficient of component i. $\Delta G^0_{(n)}$ equals the standard Gibbs energy for the reaction presented in Equation (n), $\Delta G_{R \to H}$ equals the Gibbs energy for the change between the Raoultian and Henrian standard states, R equals the gas constant and T equals temperature.

In addition to partial pressures of oxygen, the equilibria of the oxidation reactions were considered using the CO/CO_2 -ratios corresponding the equilibria. These CO/CO_2 -ratios were calculated using equation (24) that shows the relation between the partial pressures of oxygen and the corresponding CO/CO_2 -ratios based on the chemical reaction presented in equation (23).

$$2 \, CO \, (g) + O_2 \, (g) = 2 \, CO_2 \, (g) \tag{23}$$

52

$$\frac{p_{CO}}{p_{CO_2}} = \left(\frac{e^{\frac{\Delta G^0_{(23)}}{R \cdot T}}}{p_{O_2}} \right)^{1/2} \qquad (24)$$

in which p_i represents the partial pressure of component i, $\Delta G^0_{(23)}$ equals the standard Gibbs energy for the reaction presented in equation (23), R equals the gas constant and T equals temperature.

The effect of temperature on the equilibria of the oxidation reactions was studied by drawing Ellingham-type diagrams, in which the values of $R \cdot T \cdot \ln(p_{O2})$ as a function of temperature were used to describe the equilibrium of each oxidation reaction and in which the driving force for the oxidation is larger for the reactions that are located lower in the diagrams. The values of $R \cdot T \cdot \ln(p_{O2})$ were calculated separately for each sample (*i.e.* for each charge of CRC) using the values of p_{O2} obtained from equations (19) to (22) in order to describe the dispersion of the values. Additionally, equations (25) to (28) were used to calculate the boundaries between which the process is operated.

$$\left[RT \ln p_{O_2} \right]_{Si/SiO_2} = \Delta G^0_{(5)} + RT \ln a_{SiO_2} - RT \ln a_{Si} \qquad (25)$$

$$\left[RT \ln p_{O_2} \right]_{C/CO} = \Delta G^0_{(6)} + 2RT \ln p_{CO} - 2RT \ln a_C \qquad (26)$$

$$\left[RT \ln p_{O_2} \right]_{Cr/Cr_2O_3} = \Delta G^0_{(7)} + \frac{2}{3} RT \ln a_{Cr_2O_3} - \frac{4}{3} RT \ln a_{Cr} \qquad (27)$$

$$\left[RT \ln p_{O_2} \right]_{Cr/CrO} = \Delta G^0_{(8)} + 2RT \ln a_{CrO} - 2RT \ln a_{Cr} \qquad (28)$$

For equations (25) to (28), a_i represents the activity of component i and p_i the partial pressure of component i. $\Delta G^0_{(n)}$ equals the standard Gibbs energy for the reaction presented in Equation (n), R equals the gas constant and T equals temperature.

The boundaries were obtained by defining the lines representing the maximum and minimum values of $R \cdot T \cdot \ln(p_{O2})$. The maximum values were defined by using the highest values of oxide activities (*i.e.* a_{SiO2}, p_{CO}, a_{Cr2O3} and a_{CrO}) and the lowest values of element activities (*i.e.* a_{Si}, a_C and a_{Cr}) in equations (25) to (28), whereas the minimum values were achieved by using the highest values of element activities and the lowest values of oxide activities. In addition

to maximum and minimum, a line describing the oxidation of pure elements into pure oxides (i.e. $a_{SiO2} = p_{CO} = a_{Cr2O3} = a_{CrO} = a_{Si} = a_C = a_{Cr} = 1$) was also drawn for comparison.

Thermodynamic values needed for the calculations were calculated by using quadratic formalism by Ban-Ya (1993) and Xiao *et al.* (2002) for the slag phase and unified interaction parameter formalism by Pelton & Bale (1986) for the metal phase. Values for standard Gibbs energies were obtained from the databases of thermodynamic software FactSage (Bale *et al.* 2007) and HSC Chemistry (Roine 2006), whereas the values of interaction parameters were taken from the paper by Sigworth & Elliott (1974). Temperatures as well as slag and metal compositions required for the computations were measured from the CRC process of the Outokumpu Stainless Tornio works. Partial pressure of carbon monoxide was estimated based on the ferrostatic pressure inside the CRC process. More detailed descriptions concerning the values, models and assumptions used in the modelling are presented in Supplements V and VI of this thesis.

Liquid-gas -reactions: Nitrogen absorption and desorption

A computational model for absorption and desorption of nitrogen into the stainless steel melt during the AOD process has been developed in order to improve the nitrogen control. The model is based on the mass transfer equations as well as equations describing the surface area between the steel melt and bubbles, the composition of the melt in the interphase and the equilibrium between the nitrogen contents in steel and gas phases. It predicts the final nitrogen content of the steel melt in the AOD process based on the initial melt composition (Fe, Ni, Cr, O, N and S), used charge materials and process gases.

Equilibrium contents of nitrogen in the stainless steel melt as a function of steel and gas compositions were needed as boundary conditions for the above mentioned model. To simplify the overall model (and thereby shorten the times of calculation), chemical equilibria were first determined separately, after which a simplified model describing the equilibria on a limited concentration area was created based on the results of more comprehensive computations.

Firstly, nitrogen content of the stainless steel melt in equilibrium with Ar-N_2-gas was calculated. The effect of the most relevant alloying elements and impurities (*i.e.* Cr, Ni, O, S, Mo, Cu, Mn and C) was studied separately using average contents of these elements in the austenitic stainless steels as initial values. The results of these calculations indicated that the most significant

54

elements affecting the equilibrium content of nitrogen in the melt are chromium and nickel that exist in the melt with remarkably higher contents (17 wt-% and 8 wt-%, respectively) than the other elements. Therefore it was decided that the simplified model to be used in the final nitrogen model would only include the effects of chromium and nickel contents of steel melt as well as the effect of the nitrogen partial pressure on the equilibrium content of nitrogen in the steel melt.

The equilibrium compositions of the molten stainless steel in contact with Ar-N_2-gas were calculated using a computational thermodynamic software FactSage Version 5.4 and its databases (Bale *et al.* 2006). Only possible phases considered in all the calculations were a gas phase that was assumed to behave ideally and a molten steel phase that was described by an associate model of Jung *et al.* (2004) included in the FactSage databases. More detailed descriptions of the components and species considered in the computations as well as conditions (temperature, pressure, initial composition) used in the computations are presented in Supplement II of this thesis.

Reactions involving only liquid phases: Metal-slag -equilibria

Computationally obtained values describing the metal-slag -equilibria of the reactions presented in equations (13) to (15) were compared with process data measurements in order to study, whether the oxidation reactions of silicon, carbon and chromium are in mutual equilibrium at the end of the CRC process or not.

The relations between a_{Cr2O3} and X_{Si}, a_{SiO2} and X_C as well as a_{Cr2O3} and X_C were calculated using equations (29) to (31), that were obtained from the equations (16) to (18), respectively. In order to describe the dispersion of the values, the relations between a_{Cr2O3} and X_{Si}, a_{SiO2} and X_C as well as a_{Cr2O3} and X_C were calculated separately for each sample (*i.e.* for each charge of CRC) using measured measured metal and slag compositions as initial values. Quadratic formalism by Ban-Ya (1993) and Xiao *et al.* (2002) was used to calculate the actitivities of the slag components based on the measured compositions.

$$a_{Cr_2O_3} = \sqrt{\frac{a_{SiO_2}^3 \cdot f_{Cr}^4 \cdot X_{Cr}^4}{f_{Si}^3 \cdot X_{Si}^3} \cdot e^{\frac{\Delta G_{(13)}^0 + \Delta G_{R \to H}}{R \cdot T}}}$$

$$(29)$$

$$a_{SiO_2} = \frac{p_{CO}^2 \cdot f_{Si} \cdot X_{Si}}{f_C^2 \cdot X_C^2} \cdot e^{\frac{\Delta G_{(14)}^0 + \Delta G_{R \to H}}{R \cdot T}}$$

$$(30)$$

55

$$a_{Cr_2O_3} = \frac{p_{CO}^3 \cdot f_{Cr}^2 \cdot X_{Cr}^2}{f_C^3 \cdot X_C^3} \cdot e^{\frac{\Delta G_{(15)}^0 + \Delta G_{R \to H}}{R \cdot T}}$$

(31)

In equations (29) to (31), a_i represents the activity of component i, p_i the partial pressure of component i, X_i the mole fraction of component i and f_i the activity coefficient of component i. $\Delta G^0_{(n)}$ equals the standard Gibbs energy for the reaction presented in Equation (n), $\Delta G_{R \to H}$ equals the Gibbs energy for the change between the Raoultian and Henrian standard states, R equals the gas constant and T equals temperature.

In addition to the above-mentioned quadratic formalism (Ban-Ya 1993, Xiao *et al.* 2002) that was used to calculate the activities of the slag components, unified interaction parameter formalism by Pelton & Bale (1986) was used to model the metal phase. Values for standard Gibbs energies were obtained from the database of thermodynamic software HSC Chemistry (Roine 2006), whereas the values of interaction parameters were taken from the paper by Sigworth & Elliott (1974). Slag and metal compositions required for the computations were measured from the CRC process of the Outokumpu Stainless Tornio works. Partial pressure of carbon monoxide was estimated based on the ferrostatic pressure inside the CRC process. More detailed descriptions concerning the values, models and assumptions used in the modelling are presented in Supplement V of this thesis.

Reactions involving solid phases: Reactions with the lining materials

Melting and solidification behaviours of AOD and CRC slags as well as CRC slags with burned dolomite addition were estimated with thermodynamic computations. The results of these computations were compared with experimental measurements of solidus and liquidus temperatures executed with optical dilatometer as well as with SEM-EDS analyses of the experimental samples.

The melting/solidification -behaviour (*i.e.* solidus and liquidus temperatures as well as thermodynamically stable phases in different temperatures) were calculated using a computational thermodynamic software FactSage Version 5.1 and its databases (Bale *et al.* 2001). In addition to pure substances, the following solutions were taken into account in computations: liquid slag, spinel, melilite,

orthopyroxene, wollastonite, olivine, mono oxide and corundum. Models for all these phases were from the database of the used software (Bale *et al.* 2001). More detailed descriptions of the components and species considered in the computations, conditions (temperature, pressure, initial composition) used in the computations as well as experimental procedures are presented in Supplement I of this thesis.

4.1.2 Reaction rates

Although thermodynamic modelling enables to define the chemical equilibria for the reactions taking place in the AOD and CRC processes, it gives no information concerning the rates and mechanisms of these reactions. Although the focus of this thesis is in thermodynamic modelling, it is necessary to have a brief outlook on reaction rates in order to have more comprehensive view on the modelling of chemical reactions.

Reaction kinetics: Decarburization rates

Studies concerning the decarburization rates of Fe-Cr-melts with a top blown oxygen have shown that the decarburization phenomenon can be classified into two separate stages, during which the decarburization rates can be modelled by using equations (32) and (33), respectively (Kitamura *et al.* 1986):

$$-\frac{d[\%C]}{dt} = \alpha \tag{32}$$

$$-\frac{d\log[\%C]}{dt} = \beta \tag{33}$$

in which [%C] is the carbon content of the metal (in wt-%), t equals time and α and β are condition-specific constants. At the beginning of the decarburization (*cf.* equation (32)) the carbon content of the metal is still high and during this first stage the decarburization rate is increased with increased oxygen supply and increased bath stirring intensity. At the same time, the oxidation of chromium is also increased with increased oxygen supply, but decreased with increased stirring intensity. Below the critical carbon content the decarburization is controlled by mass transfer of carbon and the equation (32) is no longer valid. During this

second stage equation (33) is used to model the decarburization rates. At this stage both decarburization and oxidation of chromium are increased with increased oxygen supply and stirring intensity. (Kitamura *et al.* 1986)

Interfacial phenomena: Nitrogen absorption and desorption

Unlike the oxidation and reduction reactions which can be modelled using computational thermodynamics with tolerable accuracy, a thermodynamic model, that describes the effects of metal compositions and partial pressures of nitrogen in the gas bubbles on the nitrogen solubility of the stainless steel melts, is not sufficient for the modelling of nitrogen. Although it is important to recognize chromium's increasing effect and nickel's decreasing effect on the nitrogen solubility, it is necessary also to model the mass and heat transfer in the gas-metal systems. Since the mechanisms of both nitrogen absorption (i.e. nitrogen pick-up) and desorption (i.e. nitrogen removal) can occur in either single-site or dual-site mechanism depending on the amount of surface active elements in the metal (*cf.* chapter 3.1.1), it is necessary to model the influences of these surface active elements such as oxygen and sulphur on the interfacial properties, nitrogen absorption and desorption rates and furthermore on the nitrogen content of the metal. (*e.g.* Heikkinen & Fabritius 2012, Järvinen *et al.* 2009, Kärnä *et al.* 2008, Riipi & Fabritius 2007)

Nitrogen absorption and desorption in pure iron and iron alloys in high temperatures may be modelled by using equations (34) and (35):

$$\frac{dC}{dt} = k_1 \frac{A_{eff}}{V}(C_e - C) \tag{34}$$

$$\frac{dC}{dt} = k_2 \frac{A_{eff}}{V}(C_e^2 - C^2) \tag{35}$$

in which k_1 is the first-order rate constant, k_2 is the second-order rate constant, A_{eff} is the effective surface area of reaction, V is the volume of melt, C is the concentration of the considered element (*i.e.* nitrogen) in the melt at time t and C_e is the equilibrium concentration of the considered element in the melt at time t. The absorption of nitrogen is a dominating phenomenon during the first decarburization stages in the AOD process and its rate is calculated using the first-order equation (34). Second-order equation (35) is used to calculate the

desorption rate which is a dominant during the last stage of decarburization and during the reduction stage.

4.2   Validation of computational thermodynamics

The results of computational thermodynamics, or any other modelling, cannot be trusted unless they are validated with the results obtained by other methods.

Computations concerning the oxidation of silicon, carbon and chromium as well as metal-slag -equilibria in the CRC process were compared with the analyses of industrial samples from Outokumpu Stainless's CRC converter. Both metal and slag samples were taken manually from tilted CRC. Metal samples were taken through slag with a lollipop type sampling probe, whereas slag samples were taken with an iron rod. All the samples for the research presented in the Supplement V of this thesis were taken at the end of the blowing. For the research presented in the Supplement VI, intermediate samples were taken in addition to the final samples. Carbon contents of metal samples were analyzed with optical emission spectrometer (ARL-4460) and other elements with X-ray fluorescence (XRF; Panalytical Axios Advanced). Grinded slag briquettes were analyzed with a similar XRF as steel samples.

Results of thermodynamic computations concerning the solubility of nitrogen in stainless steel melts were compared with values of solubility presented in the literature (Jiang *et al.* 2005, Small & Pehlke 1968, Turnock & Pehlke 1966), whereas the results of the overall model were validated with the analyses of industrial samples from Outokumpu Stainless's AOD converter.

Results of computations concerning the solidification and melting behaviour of AOD and CRC slags were compared with the experimental results obtained with optical dilatometer and with SEM-EDS analyses of the samples. More detailed description of the experimental analyses is presented in Supplement I of this thesis as already mentioned in chapter 4.1.1.

4.3   Computational thermodynamics as a part of process modelling

Creation of a complete process model requires knowledge concerning thermodynamics, reaction rate kinetics as well as interfacial and transport phenomena. By combining phenomenon-based submodels describing these phenomena, comprehensive process models may be built to describe entire unit operations such as AOD and CRC processes.

As opposed to phenomenon-based models, in which each phenomenon is considered separately, process models aim for more holistic approach. Because the combination of several very detailed submodels often creates slow and non-robust models that usually are not very useful, the accuracy of describing an individual phenomenon with a larger process model is usually not as high as it is in the phenomenon-based models. On the other hand, the process models are usually more adaptable to real processes and in some cases they may be used as a part of control and automation systems. A typical feature for many process models is, that in order to be able to model the relevant phenomena by using appropriate submodels, it is necessary to define certain parameters which are required for the modelling but are not measurable or otherwise known. These kind of parameters are often used to fit the models to better correspond with the real processes. For instance, one might need to know what is the bubble size and bubble size distribution in order to calculate the mass transfer between the molten metal and the gas phase. However, the bubble size distribution inside the converter is difficult to measure and therefore the modeller needs to be satisfied with estimated values. By trying different bubble sizes and bubble size distributions, it is possible to adjust the model in order to make it more equivalent with the reality. (Heikkinen & Fabritius 2012, Järvinen *et al.* 2011)

Process models may be constructed in various ways based on their purpose and usually the phenomena that are considered to be most critical on the process optimization are modelled in greatest detail (*e.g.* chemical equilibrium, reaction kinetics, mass transfer, fluid flows, heat transfer, interfacial phenomena, and so on). This means that separate researchers may end up with very different kind of models based on the target of their modelling as well as on their own impressions. In addition to what is included in the process models and in which extent and accuracy, the models may also differ from one another based on the connections that link the submodels with each other. (Heikkinen & Fabritius 2012)

Process models for the AOD converter have been proposed by *e.g.* Fruehan (1976), Sjöberg (1994), Wei & Zhu (2002), Zhu *et al.* (2007), Wei *et al.* (2011), Järvinen *et al.* (2011), Visuri *et al.* (2013a, 2013b) and Andersson *et al.* (2013).

One of the most fundamental tasks of an AOD process model - and hence one of the things that is most often modelled with these models - is to determine how oxygen is consumed in the process. Oxygen consumption may be presented with the concept of carbon removal efficiency which describes what is the proportion of blown oxygen that reacts with carbon during the decarburization as presented in equation (36). (*e.g.* Swinbourne *et al.* 2012, Visuri *et al.* 2013a, Wijk 1992)

$$CRE(\%) = \frac{Amount\ of\ oxygen\ reacting\ with\ carbon}{Total\ added\ oxygen} \cdot 100 \qquad (36)$$

According to *e.g.* Andersson *et al.* (2013), the values of CRE may vary very drastically (*i.e.* between 5 % and 95 %) during the AOD process.

5 Results

The purpose of this chapter is to present the results of computational thermodynamics used in the research and development of AOD and CRC converters within the case studies presented in Supplements I, II, III, V and VI of this thesis. The results are presented in three categories (*cf.* Figure 4 in chapter 1.2): studies that involve reactions between molten metal and gas (chapter 5.1), studies focusing only on reactions between liquid phases (chapter 5.2; Supplement V) and studies in which reactions involving solid phases are being considered (chapter 5.3; Supplement I). Furthermore, the liquid-gas -reactions presented in chapter 5.1 are divided into two separate studies: the oxidation of silicon, carbon and chromium in the CRC process (chapter 5.1.1; Supplements V and VI) and nitrogen in stainless steel melts of the AOD process (chapter 5.1.2; Supplements II and III).

5.1 Liquid-gas -reactions

5.1.1 Oxidation of silicon, carbon and chromium

Oxidation reactions of silicon, carbon and chromium in the CRC process were considered by comparing the results of computational thermodynamics with process samples from the Outokumpu Stainless Tornio steelworks.

Calculated partial pressures of oxygen corresponding to the equilibria between measured Si- and SiO_2-contents, measured C-contents and estimated partial pressure of CO as well as measured Cr- and Cr_2O_3/CrO-contents are presented in Figure 11. Concerning the notation in Figure 11, '1' represents intermediate samples, whereas '2A' and '2B' respresent final samples from two different kind of charges. Samples '2A' were taken from charges in which low-carbon ferrochromium was produced and additional silicon was added to metal in order to enhance its crushability, since it could not be directly charged into the AOD process. Samples '2B' were taken from the charges in which no additional silicon was added (*i.e.* direct charging to the AOD process).

In order to be in mutual equilibrium with each other, the partial pressures of oxygen calculated for the oxidation reactions of silicon, carbon and chromium should have values that are close to one another.
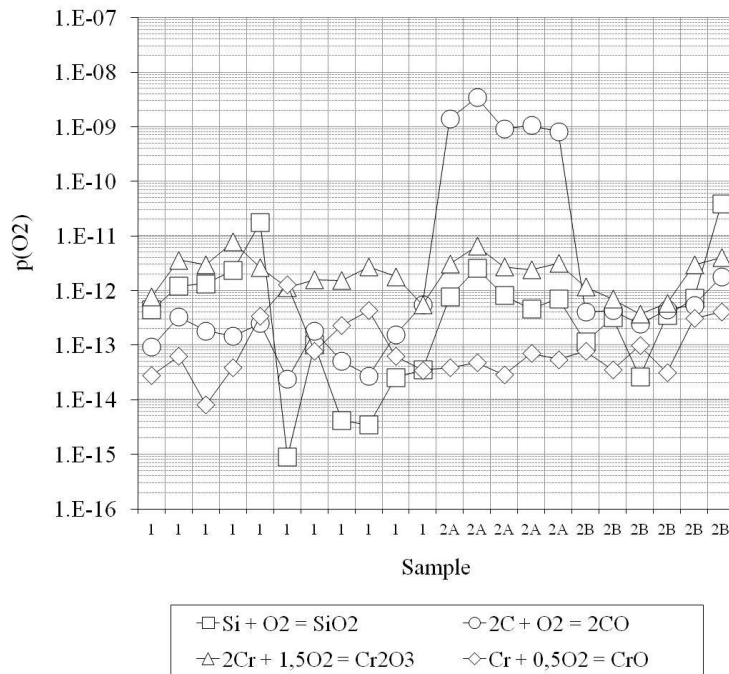
Fig. 11. Partial pressures of oxygen calculated from the measured process data concerning the slag and metal compositions at the different stages of the blowing.

It is seen from Figure 11 that for intermediate samples (marked with '1' in Figure 11) as well as for final samples with silicon addition (marked with '2A' in Figure 11) the difference between the partial pressures of oxygen describing the equilibria of different oxidation reactions is significant (up to three or four decades), although there are few samples in which the difference between the values of p_{O2} is considerably lower (especially if one assumes that chromium is oxidized into CrO and not into Cr_2O_3). This indicates that the oxidation reactions of silicon, carbon and chromium are generally not in mutual equilibrium, although it is close in some individual charges. The mutual equilibrium of the oxidation reactions is most likely achieved in charges in which no additional silicon was added (samples marked with '2B' in Figure 11), although even these samples show some variation in the values of p_{O2}. The variation is largest (*i.e.* the oxidation reactions are least likely to be in mutual equilibrium with each other) in samples '2A' which represent the charges in which additional silicon was added to the melt after the blowing. However, rather than the silicon addition itself, the

63

reason for the difference is more likely to be the lower carbon content in the metal in these samples, since higher partial pressures of oxygen (*i.e.* more oxidizing conditions) are required to oxidize carbon when its content decreases.

In addition to mutual equilibrium, it is possible to estimate the order of oxidation for silicon, carbon and chromium by comparing the partial pressures of oxygen that are needed to oxidize these elements. According to Figure 11 it seems that for intermediate samples (once again marked with '1') the order of oxidation is either $Si \rightarrow C \rightarrow Cr$ (to CrO) $\rightarrow Cr$ (to Cr_2O_3) or Cr (to CrO) $\rightarrow C \rightarrow Si \rightarrow Cr$ (to Cr_2O_3) depending the amounts of silicon and carbon in the metal. This order indicates that chromium does not necessarily oxidize to Cr^{3+} (Cr_2O_3), if the oxidizing conditions are assumed to be determined by the oxidation reactions of silicon and/or carbon.

Due to additional silicon addition, the order of oxidation is more difficult to define for the final samples. For the samples '2B' (*i.e.* no silicon addition) the order of oxidation seems to be Cr (to CrO) $\rightarrow Si/C \rightarrow Cr$ (to Cr_2O_3), although the difference between the values of p_{O2} describing the formation of Cr_2O_3, SiO_2 and CO is not very clear. This indicates that the chromium is more likely to have a higher valence (Cr^{3+}) in final samples than in the intermediate ones. The order of oxidation for the samples '2A' (in which silicon was added to the charge) is Cr (to CrO) $\rightarrow Si \rightarrow Cr$ (to Cr_2O_3) $\rightarrow C$, which reflects the difficulties to achieve low carbon contents without oxidizing the chromium.

The results concerning the order of oxidation at different stages of the CRC process are summarized in Table 9.

Table 9. Order of oxidation at different stages of the CRC process.

Stage		Order of oxidation			
During the blowing		Si	C	Cr (to Cr^{2+})	Cr (to Cr^{3+})
	or	Cr (to Cr^{2+})	C	Si	Cr (to Cr^{3+})
After the blowing		Cr (to Cr^{2+})	Si and C	Cr (to Cr^{3+})	
After the blowing and Si-addition		Cr (to Cr^{2+})	Si	Cr (to Cr^{3+})	C

In addition to partial pressures of oxygen, the mutual equilibrium of the oxidation reactions was considered using the CO/CO_2 -ratios corresponding the equilibria as mentioned in chapter 4.1.1. This consideration is presented in Figure 12. In addition to the conclusions that could already be drawn from Figure 11, it is seen from Figure 12 that even though the difference between the CO/CO_2 -ratios (or partial pressures of oxygen as seen from Figure 11) can be relatively large (up to

several decades), it does not necessarily require big amounts of CO_2 to change the CO/CO_2 -ratio quite drastically, since the equilibrium is heavily on the CO's side.
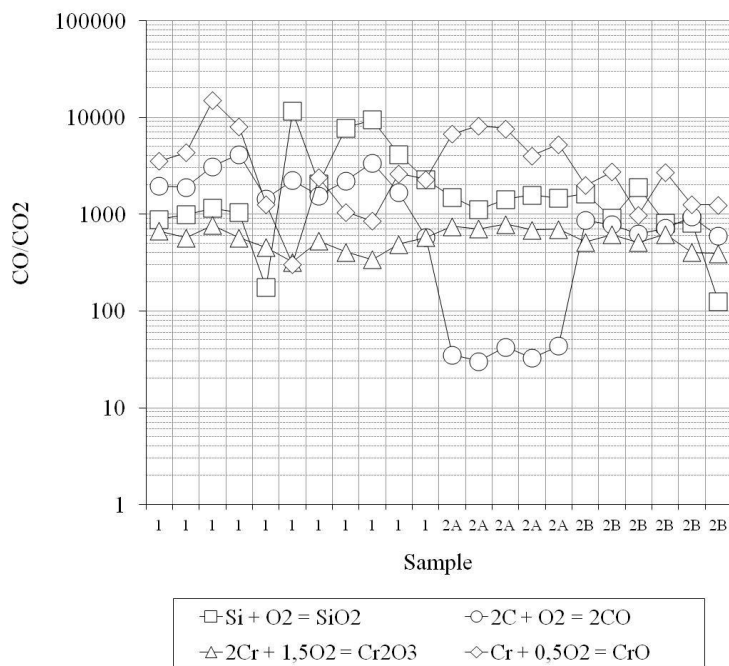
Fig. 12. CO/CO$_2$-ratios calculated from the measured process data concerning the slag and metal compositions at the different stages of the blowing.

The effect of metal composition on the state of equilibrium of the oxidation reactions is presented in Figures 13 to 15, in which the partial pressures of oxygen representing the equilibrium of the oxidation reactions of silicon, carbon and chromium (*i.e.* reaction presented in equations (5) to (8)) are plotted as a function of silicon, carbon and chromium contents in the metal.

In Figure 13 it is shown that the partial pressure of oxygen in equilibrium with Si and SiO_2 depends strongly on the metal's silicon content, since the amount of oxygen needed to oxidize silicon increases when the silicon content in metal decreases. The higher values of p_{O2} in the silicon content range of 6-9 mol-% (samples '2A') are due to silicon addition at the end of the blowing and therefore these points are not comparable with the others.
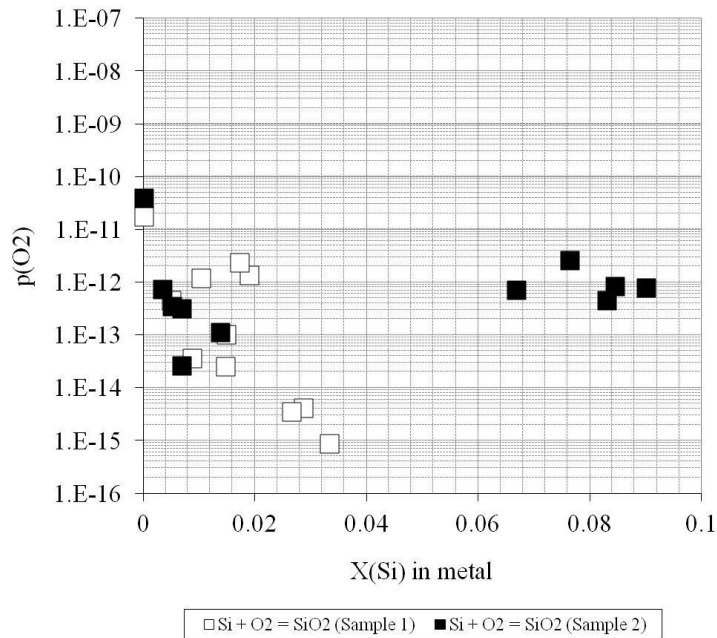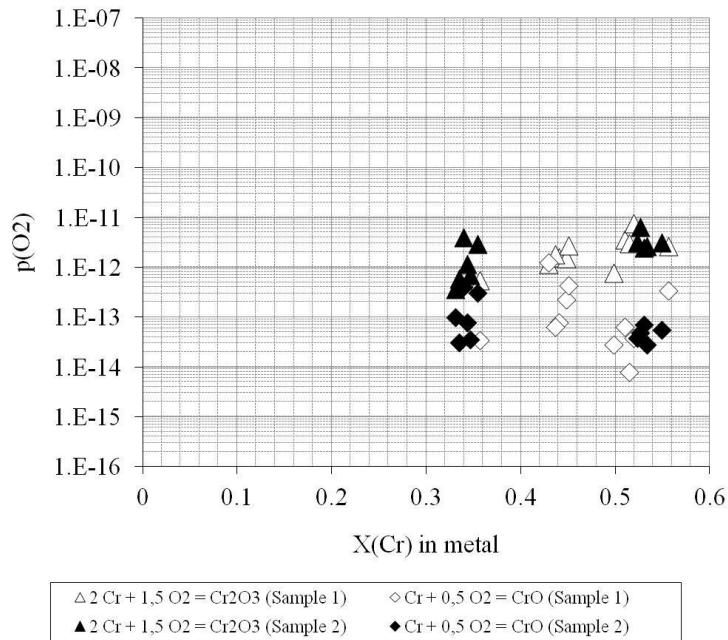
Fig. 13. Partial pressures of oxygen representing the equilibrium between silicon (in metal) and SiO$_2$ (in slag) as a function of silicon content in metal calculated from the measured process data concerning the slag and metal compositions at the different stages of the blowing.

A behavior similar to silicon can be observed from Figure 14 for the equilibrium between carbon and carbon monoxide. With higher carbon contents (*i.e.* the intermediate samples '1') the partial pressure of oxygen needed to oxidize the carbon is low, but it increases as metal's carbon content decreases during the blowing. In the final samples (*i.e.* samples '2') the values of p_{O2} describing the C-CO-equilibrium are higher the further the decarburization proceeds. Since no extra carbon is added to the metal after the blowing, all the final samples are comparable unlike in Figure 13.
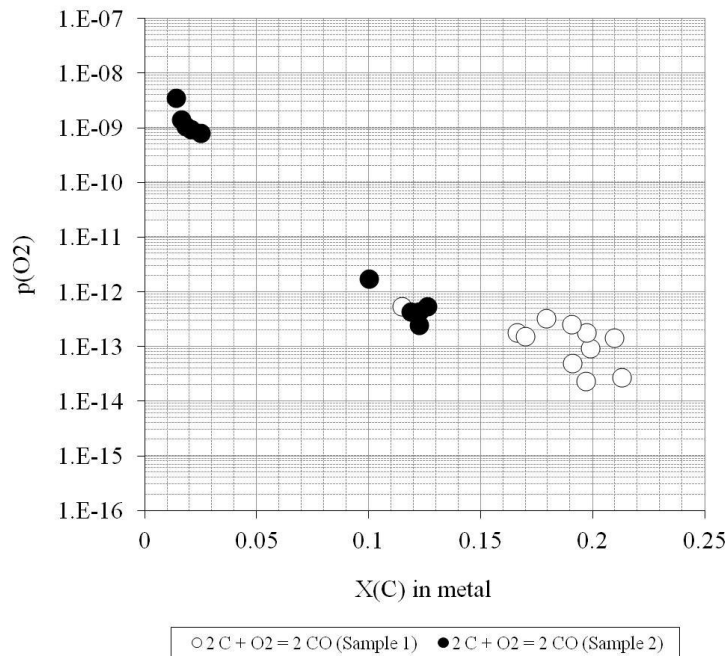
Fig. 14. Partial pressures of oxygen representing the equilibrium between carbon (in metal) and carbon monoxide (gas) as a function of carbon content in metal calculated from the measured process data concerning the metal compositions at the different stages of the blowing.

Figure 15 is not as informative as Figures 13 and 14. Due to high chromium content in the molten metal during all the stages of blowing, the partial pressure of oxygen needed to oxidize the chromium into either CrO or Cr_2O_3 did not vary much as a function of blowing time nor as a function of chromium content. Hence the behavior typical to oxidation of silicon and carbon as seen in Figures 13 and 14 is not observable for the chromium (this would require samples with a much lower chromium content in the metal). Figure 15 also shows that the formation of CrO requires less oxidizing conditions in comparison to the formation of Cr_2O_3, although this is rather obvious since chromium has a lower valence in CrO and higher in Cr_2O_3.

Fig. 15. Partial pressures of oxygen representing the equilibrium between chromium (in metal) and either Cr$_2$O$_3$ or CrO (both in slag) as a function of chromium content in metal calculated from the measured process data concerning the slag and metal compositions at the different stages of the blowing.

As it was already considered in the context of Figure 11, the calculated partial pressures of oxygen presented in Figures 13 to 15 can also be used to estimate the order of oxidation for silicon, carbon and chromium at the different stages of blowing. It is seen from Figures 13 to 15 that with higher silicon contents the driving force for the oxidation of silicon is greater than the one of carbon and chromium (*i.e.* the partial pressures of oxygen describing the equilibrium between carbon and CO as well as chromium and CrO or Cr$_2$O$_3$ in Figures 14 and 15 are higher than the ones describing the equilibrium between silicon and SiO$_2$ in Figure 13). However, as the silicon content in metal decreases towards the end of blowing, the driving force for the oxidation of carbon and chromium becomes greater. As the decarburization proceeds, the partial pressure of oxygen needed to oxidize the carbon into CO increases, too, thus making the driving force for the oxidation of chromium greater than the ones for either silicon or carbon.

According to Figures 14 to 15, the partial pressures of oxygen required to oxidize chromium and carbon are approximately 10^{-13} for chromium into CrO, approximately 10^{-12} for chromium into Cr_2O_3 and approximately 10^{-13} for carbon into CO with higher carbon contents in metal. On the other hand, Figure 13 shows that the values of p_{O2} describing the equilibrium between silicon and SiO_2 exceed 10^{-13}-10^{-12} when the mole fraction of silicon in metal decreases below 0.004-0.010. Hence, the silicon content below which it becomes more favourable for chromium and carbon to be oxidized in comparison to silicon, is approximately 0.4-1.0 mol-% (*i.e.* 0.29-0.62 wt-%). Observations from the CRC process have indicated that the oxidation of chromium becomes significant when the silicon content of the metal decreases below 0.1 wt-%.

Figures 14 and 15 also illustrate, that since the oxidation of chromium increases below the carbon contents of approximately 10 mol-% (*i.e.* 2.5 wt-%), the reduction of chromium is required when producing ferrochromium with carbon contents lower than this.

As mentioned in chapter 4.1.1, the effect of temperature on the equilibria of the oxidation reactions was studied by using Ellingham-type diagrams. In these diagrams (presented in Figures 16 to 19) the values of $R \cdot T \cdot \ln(p_{O2})$ as a function of temperature were used to describe the equilibrium of each oxidation reaction. Driving force for oxidation is larger for the reactions that are located lower in the diagrams. In this study the values of $R \cdot T \cdot \ln(p_{O2})$ were calculated separately for each charge of the CRC process that was considered in this study. Additionally, the boundaries between which the process is operated were calculated, too. These boundary values for $R \cdot T \cdot \ln(p_{O2})$ are illustrated in Figures 16 to 19 as thick lines with diamonds, whereas thick lines with squares illustrate the oxidation of pure elements into pure oxides. Open circles as well as open triangles represent the values calculated for individual intermediate samples (*i.e.* samples '1'), whereas closed circles represent individual final samples with a silicon addition (*i.e.* samples '2A') and closed triangles individual final samples without a silicon addition (*i.e.* samples '2B'). Thin lines are drawn to represent the values of p_{O2} at intervals of two decades the uppermost corresponding the value of 10^{-8} and the lowest corresponding the value of 10^{-18}.
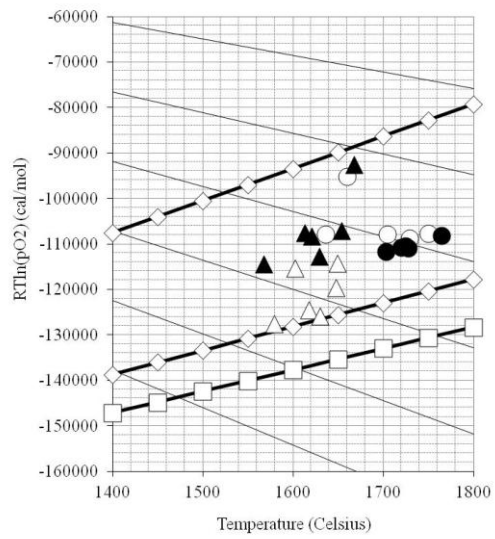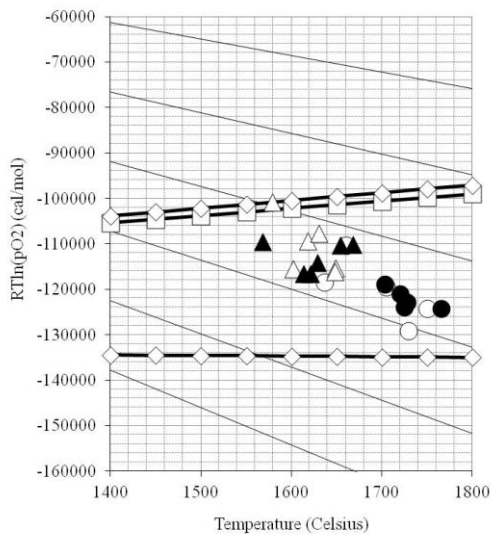
Fig. 16. Ellingham-type diagram for the Si/SiO₂ -equilibrium.
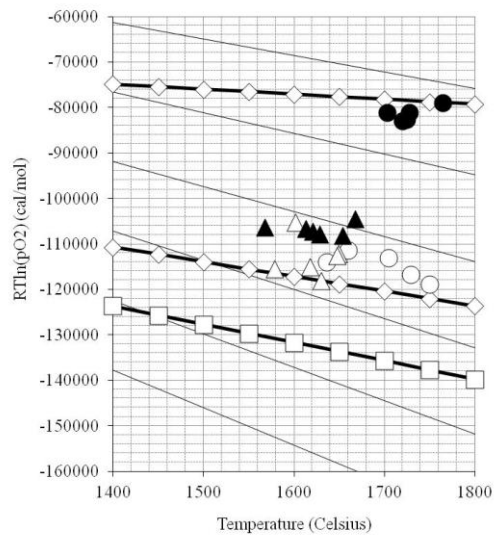
Fig. 17. Ellingham-type diagram for the C/CO -equilibrium.
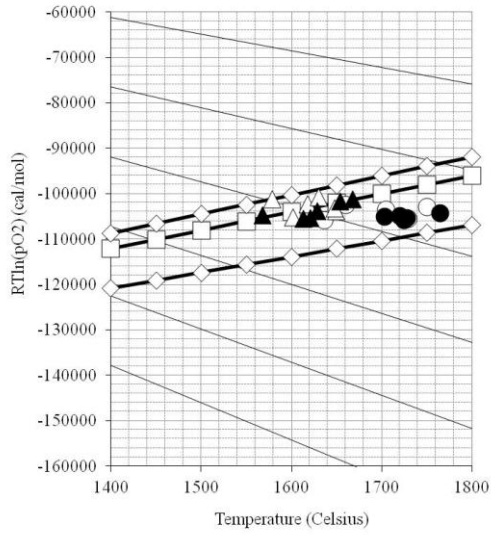
Fig. 18. Ellingham-type diagram for the Cr/Cr$_2$O$_3$ -equilibrium.

Fig. 19. Ellingham-type diagram for the Cr/CrO -equilibrium.

Figures 16 to 19 show that although there are considerable variations in the temperatures of different samples, it is difficult to separate out the actual effect of temperature on the reaction equilibria, since it is not the only changing variable in the samples. This is clearly seen in Figure 17 which shows that the equilibrium between carbon and carbon monoxide is totally different in samples '2A' (closed circles) and in samples '1' (open circles) even though they appear in the same temperature range. This indicates that the equilibria are more dependent on the metal and slag compositions than on temperature. Nevertheless, Figure 19 shows some indication on the temperature dependence of the Cr/CrO -equilibrium.

5.1.2 Nitrogen absorption and desorption

Nitrogen solubilities in stainless steel melts as a function of steel and gas compositions were determined with computational thermodynamics in order to create a thermodynamic submodel for an overall model that was used to estimate the nitrogen content of the metal in the AOD process.

In the first part of computations, the effects of chromium, nickel, oxygen, sulphur, molybdenum, copper, manganese and carbon on nitrogen solubility were studied separately. The contents of these elements were chosen to correspond average contents in austenitic stainless steels and are presented in the Supplement II of this thesis.

The influences of oxygen (0.04 wt-%) and sulphur (0.025 wt-%) on the nitrogen contents of iron-based metals containing 17 wt-% of chromium as well as 17 wt-% of chromium and 8 wt-% of nickel as a function of gas composition at 1700 °C are presented in Figure 20.

Figure 21 illustrates the influence of molybdenum, copper, manganese and carbon on the nitrogen content of an iron-based metal containing 17 wt-% of chromium and 8 wt-% of nickel as a function of gas composition at 1700 °C as well as nitrogen contents as a function of gas composition for a stainless steel including all the elements considered in this study at 1700 °C. Additionally, Figure 21 contains nitrogen solubilities of stainless steels AISI304 and AISI316L at 1580 °C according to Jiang *et al.* (2005). The compositions of AISI304 and AISI316L are presented in the Supplement II of this thesis.

72
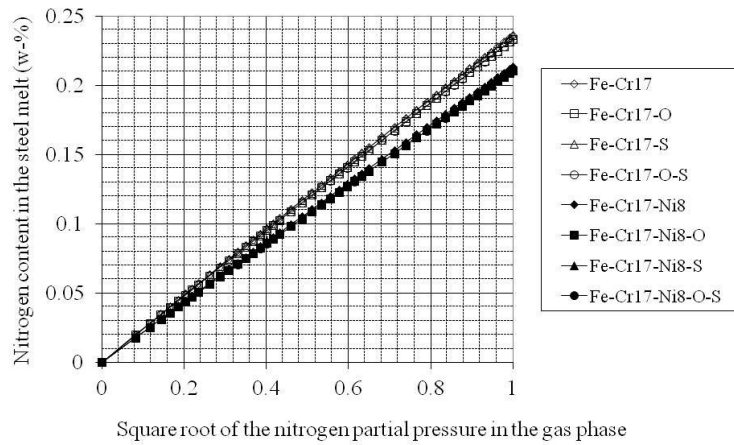
Fig. 20. The influence of oxygen and sulphur on the nitrogen contents of the Fe-Cr17- and Fe-Cr17-Ni8 -melts in equilibrium with different gas compositions at 1700 °C.

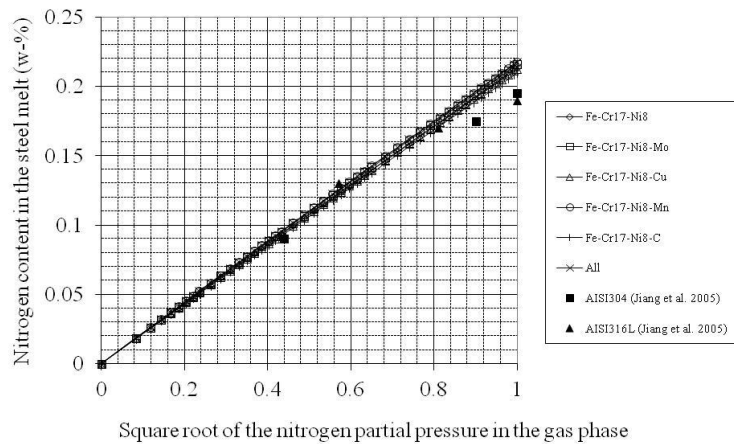**Fig. 21. The influence of molybdenum, copper, manganese and carbon on the nitrogen content of the Fe-Cr17-Ni8-melt in equilibrium with different gas compositions at 1700 °C as well as nitrogen contents as a function of gas composition for stainless steel including all the elements considered in this study at 1700 °C and for stainless steels AISI304 and AISI316L at 1580 °C according to Jiang *et al.* (2005).**

To verify the results of computations, they were compared with the values of nitrogen solubilities presented by Small *et al.* (1968) and Jiang *et al.* (2005).

Figure 22 illustrates the computational nitrogen contents in steel melts as a function of gas composition for pure iron as well as for iron-based metals containing 17 wt-% of chromium as well as 17 wt-% of chromium and 8 wt-% of nickel at 1700 °C. In addition to the results of this study, the nitrogen solubilities of iron-based metals containing 17 wt-% of chromium as well as 17 wt-% of chromium and 10 wt-% of nickel at 1600 °C presented by Small *et al.* (1968) and Jiang *et al.* (2005) are presented in Figure 22.
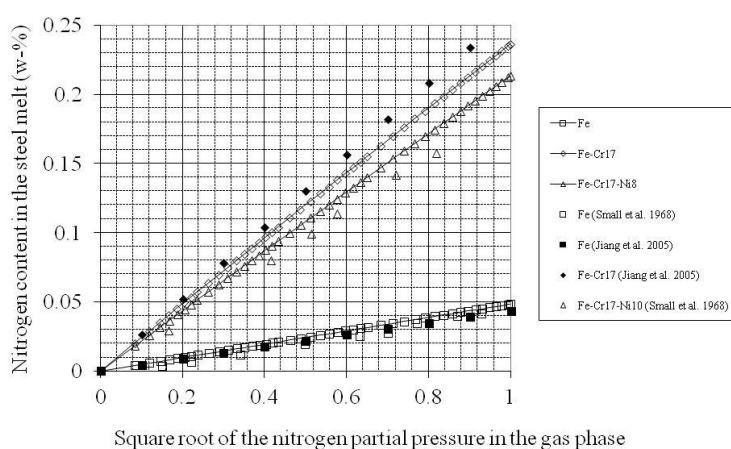
Fig. 22. Nitrogen contents in the steel melts in equilibrium with different gas compositions for pure iron, Fe-Cr17 and Fe-Cr17-Ni8 at 1700 °C, for pure iron and Fe-Cr17-Ni10 at 1600 °C according to Small *et al.* (1968) and for pure iron and Fe-Cr17 at 1600 °C according to Jiang *et al.* (2005).

The solubility of nitrogen in chromium-containing stainless steels is considerably higher than the solubility in low-alloyed steels. Although the higher nickel content in austenitic stainless steels lowers the nitrogen solubility, it is still approximately four times higher than the solubility in pure iron as seen from Figure 22. It is also seen from Figures 20-22 that the equilibrium content of nitrogen in the steel melt is (according to Sievert's law) a linear function of a square root of a partial pressure of nitrogen in the gas phase. This is correct for both pure iron and stainless steels.

74

The values for pure iron presented by Small *et al.* (1968) and Jiang *et al.* (2005) are slightly lower but nevertheless clearly in the same magnitude than the ones computed in this study. This is understandable since the effect of temperature on the solubility of nitrogen in pure iron is almost negligible in the temperature range of 1500 to 1700 °C (Jiang *et al.* 2005). The solubility of nitrogen in Fe-Cr17 -melt according to Jiang *et al.* (2005) is higher than the one computed in this study. This difference can be explained by different temperatures, since the increase in temperature decreases the solubility of nitrogen in iron-chromium melts (Jiang *et al.* 2005).

The nitrogen solubilities for Fe-Cr17-Ni10 -melt by Small *et al.* (1968) presented in Figure 22 are lower than the ones for Fe-Cr17-Ni8 -melt according to this study since the increasing nickel content decreases the solubility of nitrogen. The differences between the nitrogen contents of stainless steel melts according to this study and the ones for AISI304 and AISI316L by Jiang *et al.* (2005) (*cf.* Figure 21) can be explained by a lower chromium content (for AISI304) and a higher nickel content (for AISI316L) in Jiang's *et al.* (2005) study in comparison to this study.

It was clearly seen from Figures 20 to 22 that the contents of alloying and impurity elements (except for chromium and nickel) were too low to have a significant effect on the equilibrium content of nitrogen in stainless steel melts. Therefore it was concluded that the only factors in the overall nitrogen model to be considered to have an effect on the equilibrium content of nitrogen in the steel melt would be the contents of chromium and nickel as well as the partial pressure of nitrogen in the gas phase. Hence, the second part of computations consisted of a study in which the influence of chromium and nickel contents was considered on a composition range of 15 to 20 wt-% of chromium and 8 to 12 wt-% of nickel. Some of the results are presented as an example in Figure 23.
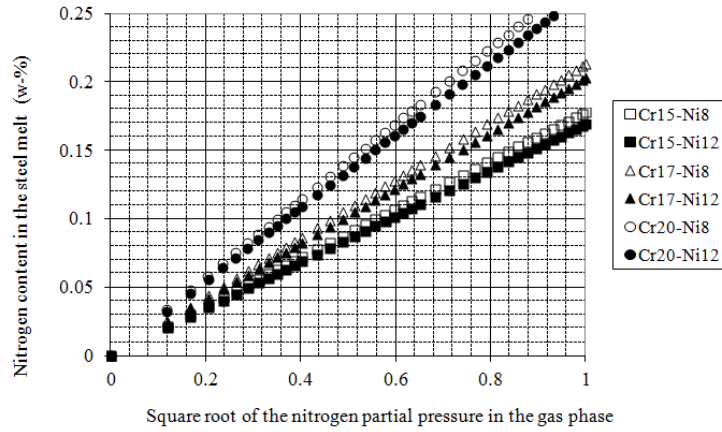
Fig. 23. The influence of chromium and nickel contents in the nitrogen content of stainless steel melt in equilibrium with gases with different nitrogen partial pressures at 1973 K.

Based on the results from the second part of computations, a simplified model describing the equilibrium amount of nitrogen in stainless steel melts as a function of chromium and nickel contents as well as partial pressure of nitrogen was created. This equation is presented in Equation (37):

$$[wt-\%]_N = \begin{bmatrix} \left(-11.8 \cdot m_{Cr}^2 + 1.81 \cdot m_{Cr} - 0.233\right) \cdot m_{Ni} \\ +9.68 \cdot m_{Cr}^2 - 1.15 \cdot m_{Cr} + 0.152 \end{bmatrix} \cdot p_{N_2}^{1/2} \tag{37}$$

in which $[wt-\%]_N$ represents the equilibrium content of nitrogen in the steel melt in wt-%, m_{Cr} and m_{Ni} represent the mass fractions of chromium and nickel in the steel melt, respectively, and p_{N2} represents the partial pressure of nitrogen in the gas phase in contact with steel.

While using the simplified model presented in Equation (37) it should be noted that the influences of many elements as well as temperature was considered to be negligible only because their variation in the system under consideration was assumed to be relatively small and therefore their influence on the nitrogen solubility not to be worthy of consideration. If the variations were larger, the influence of these factors would have to be considered in the overall model as the effect of *e.g.* temperature is significant in the solubility of nitrogen in the stainless steels (Jiang *et al.* 2005). The variation of temperature during the AOD process is

76

approximately 150 °C (between 1600 °C and 1750 °C) as is seen from Figure 7 in chapter 2.2 and it can be controlled by scrap charging.

Another thing that is worth mentioning while considering the results of computational thermodynamics is the influece of surface active elements. As seen from Figures 20 and 21, the influence of other alloying elements and impurities besides chromium and nickel on the nitrogen content of steel melt is very small. This is due to a relatively small amounts of these elements (O, S, Mo, Cu, Mn, C) in the melt. It should however be noted that even very small amounts of surface active elements such as sulphur and oxygen have a great influence on the nitrogen content of the steel melt because they are concentrated on the surfaces and therefore prevent the transfer of nitrogen from one phase to another; *i.e.* both from gas to steel melt and vice versa (*e.g.* Ito *et al.* 1988, Lee & Morita 2003, Rao & Cho 1990). This influence is not observed in thermodynamic calculations since the equilibrium considerations do not take the reaction mechanisms and kinetics into account. The influence of sulphur and oxygen on the kinetics of the nitrogen transfer through the phase boundary were modelled in the overall nitrogen model, but their influence is not based on thermodynamics and therefore not observable in the results presented in Figures 20 and 21.

On the other hand, Rao & Cho (1990) have also reported that the increase in the chromium content of the steel melt decreases the surface activity of sulphur and therefore decreases the effect of sulphur on the nitrogen transfer through the phase interface. Lee *et al.* (2005) have mentioned that this influence of chromium is based on the altered equilibrium content of oxygen which in turn has an effect on the sulphur's surface activity due to strong interactions between oxygen and sulphur.

The overall nitrogen model, in which the simplified thermodynamic model presented in Equation (37) is included, was used to predict the final nitrogen content of the steel melt in the AOD process based on the initial melt composition (Fe, Ni, Cr, O, N and S), used charge materials and process gases. In addition to thermodynamic boundary conditions the overall model contains models describing the absorption and desorption of nitrogen as a function of time as well as the equations describing the surface area between the steel melt and bubbles and the equations describing the composition of the melt in the interphase.

One example of the results is presented in Figure 24, in which the nitrogen contents as a function of blowing time obtained from the overall nitrogen model and the thermodynamic submodel are compared with the compositions of the samples taken from one AOD charge at the Outokumpu Stainless Tornio steel

plant. It is seen from Figure 24 that for the considered charge, the absorption of nitrogen is spontaneous during the first stages of blowing (until 9 minutes of blowing time), after which the desorption of nitrogen becomes spontaneous.
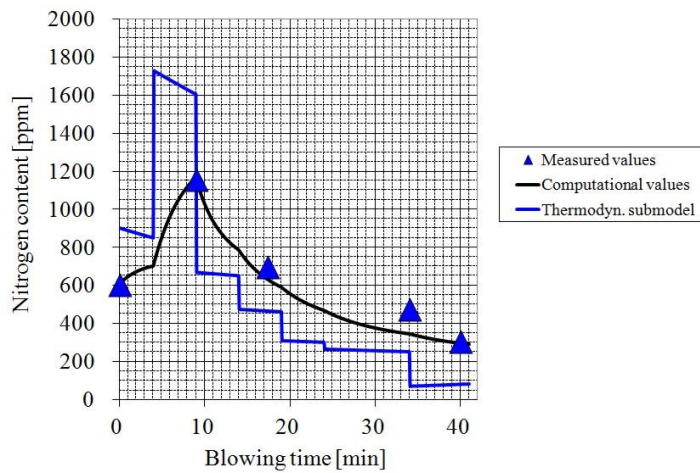
Fig. 24. Measured nitrogen contents from Outokumpu Stainless' AOD converter as well as computational nitrogen contents according to thermodynamic submodel and overall nitrogen model as a function of blowing time.

Since computational thermodynamics is only one part of the overall nitrogen model, its detailed description is omitted here as a topic that is not most relevent considering the focus of this thesis. The overall model is however presented in more detail in Supplement III of this thesis.

5.2   Reactions involving only liquid phases

The metal-slag -reactions involving silicon, carbon and chromium in the CRC process were considered by comparing the results of computational thermodynamics with slag and steel analyses measured from the samples that were taken from the Outokumpu Stainless' CRC process at the end of the blowing.

The calculated values of activities of Cr_2O_3 and SiO_2 as a function of mole fractions of silicon and carbon are presented in Figures 25 to 27 together with the measured melt compositions and calculated slag activity values from the CRC process of the Outokumpu Stainless Tornio works. Slag activities were calculated

78

by using the analysed slag compositions from Outokumpu Stainless' CRC process as initial values. Three different partial pressures of CO in Figures 26 and 27 represent the situation in three different depths in the CRC process. A more detailed description of the calculations is presented in the Supplement V of this thesis.
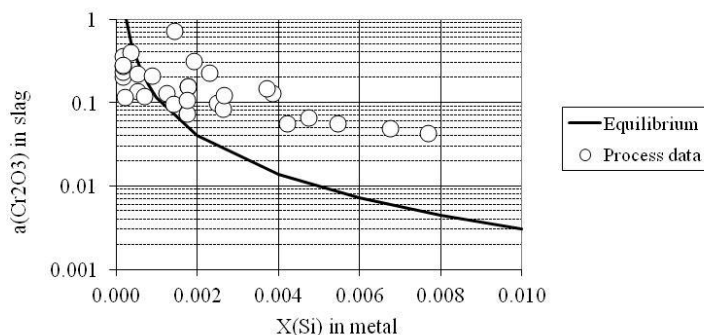
Fig. 25. Calculated activities of Cr$_2$O$_3$ in the slag as a function of silicon content in the metal as well as measured process data from the CRC process.
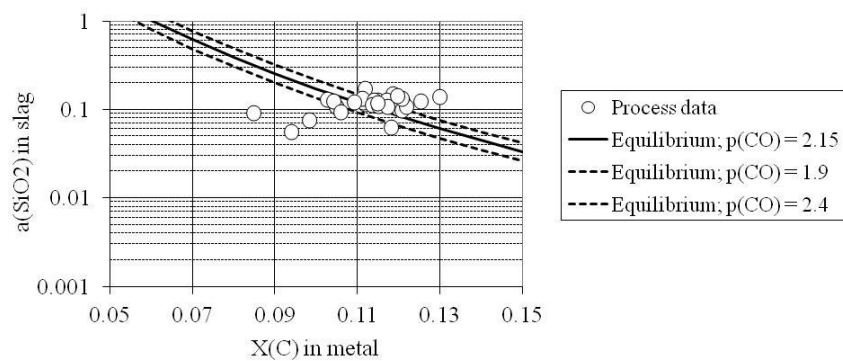
Fig. 26. Calculated activities of SiO$_2$ in the slag as a function of carbon content in the metal as well as measured process data from the CRC process.
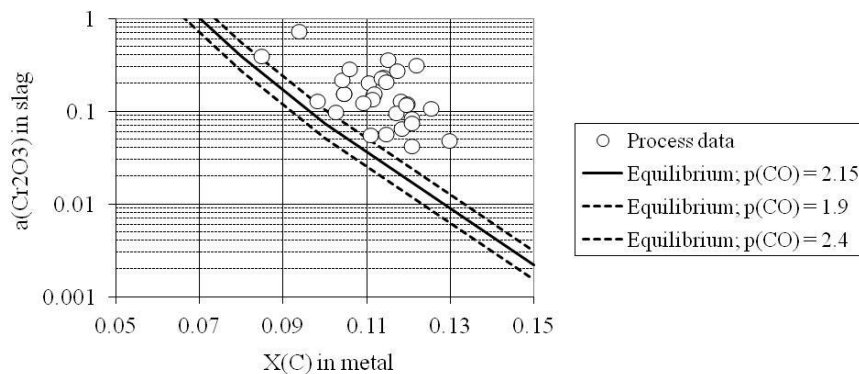
Fig. 27. Calculated activities of Cr$_2$O$_3$ in the slag as a function of carbon content in the metal as well as measured process data from the CRC process.

It is seen from Figure 25 that the activity of Cr$_2$O$_3$ in the slag depends on the metal's silicon content according to the reaction presented in equation (13). Activity of Cr$_2$O$_3$ in slag increases as the silicon content in melt is lowered (*cf.* Figure 8 in chapter 2.3). When the silicon content of the metal is close to zero (as it usually is at the end of the blowing), the calculated activity of Cr$_2$O$_3$ closes to unity. Calculated equilibrium and the measured process data are in good agreement in low but not in high silicon contents. If the used models are assumed to be valid in the considered composition range, the differences between the calculated and measured values could indicate that the CRC slag is not in thermodynamic equilibrium with the metal at the end of the blowing if the silicon content is higher. Since high silicon contents in the metal are not desirable at the end of the CRC blowing, it is possible that concerning the measurements of high silicon content there has been some sort of deviation from the normal practice due to which the equilibrium has not been reached. The most probable explanation is insufficient mixing concerning these measurements.

It is seen from Figure 26 that the deviations in the activity of SiO$_2$ as a function of the metal's carbon content are small. The relatively constant values of a$_{SiO2}$ can be explained with the additions of CaO and MgO that are used as slag modifiers to keep the slag basicity in control. In other words the activity of SiO$_2$ is determined by the slag composition controlled with CaO and MgO additions, not by the equilibrium of the reaction presented in equation (14). If SiO$_2$ activity in slag would be increased with slag composition modification, lower carbon

contents in melt could be achieved. However, the lower carbon contents of the metal would increase the oxidation of chromium as seen from Figure 27.

When considering the results presented in Figures 25 to 27, one should be aware of few significant limitations. In the calculations from which the results presented in Figures 25 to 27 were obtained the system was assumed to be isothermal and divalent chromium was not considered. Additionally, all the process samples were taken at the end of the CRC blowing as no intermediate samples were considered in this study. Due to these limitations, the results concerning the oxidation of silicon, carbon and chromium presented in chapter 5.1.1 are more likely to be accurate, since the above mentioned limitations were corrected for the calculations presented in chapter 5.1.1.

5.3   Reactions involving solid phases

Computed solidus and liquidus temperatures of the AOD and CRC slags as a function of $(MgO+CaO)/SiO_2$ -ratio are presented in Figure 28 together with experimentally measured solidus and liquidus temperatures. Liquidus temperatures of the quaternary Al_2O_3-CaO-MgO-SiO_2-system with 5 % Al_2O_3 and with CaO/MgO-ratios of 2.24 (corresponding the CRC slag) and 5.74 (corresponding the AOD slag) according to Kowalski et $al.$ (1995) are also presented in Figure 28 for comparison.

Solid phases that are formed during the solidification of AOD and CRC slags according to computations and experiments are presented in Tables 10 and 11, respectively. CRC slag with burned dolomite addition and with the $(MgO+CaO)/SiO_2$ -ratio of 2.56 was also studied experimentally, but it is ignored in Table 11, because it was not completely molten at 1700 °C, which was the maximum temperature of the experiments. Hence it was not meaningful to determine the phases that are formed during the solidification because some original solid phases were still left in the sample.

In Tables 10 and 11 the most significant solid phases are marked with bold and in Table 11 the phases with the smallest amounts are marked in italics. A column with the title 'CRC slag with burned dolomite addition' in Table 10 refers to the computations in which the CRC slag with the $(MgO+CaO)/SiO_2$ -ratio of 2.56 ($cf.$ Table 11) was considered.
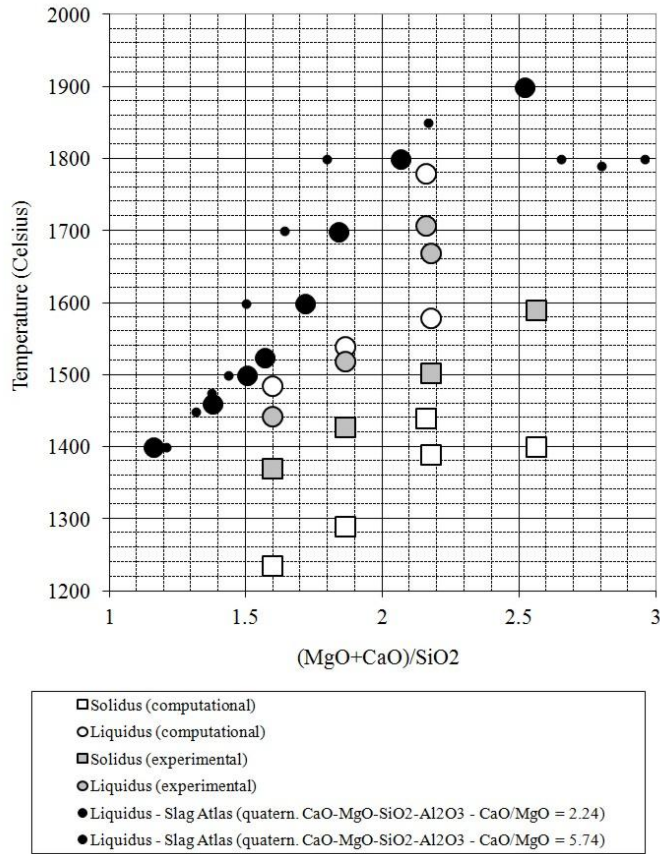
Fig. 28. The effect of (MgO+CaO)/SiO₂-ratio on the solidus and liquidus temperatures of the AOD and CRC slags.

It is seen from Figure 28 that there are considerable variations in the values of solidus and liquidus temperatures attained from the different sources (*i.e.* experiments, calculations and the literature). Some of the variations can be explained by (1) the different CaO/MgO-ratios in AOD and CRC slags (AOD slag having higher solidus and liquidus temperatures than CRC slags), (2) limited amount of components that were taken into account in the computations in comparison to the actual slags in the experiments (leading to higher liquidus temperatures in computations) and (3) difficulties in the observation of very small amounts of liquid and solid phases with the optical dilatometer (leading to higher solidus and lower liquidus temperatures in the experiments in comparison to

82

computations). Despite the inaccuracy in the actual values, the trends, which were the main focus of interest, were consistent with each other.

Table 10. Solid phases that are formed during the solidification of AOD and CRC slags according to thermodynamic computations.

T (°C)	CRC slag without burned dolomite addition	CRC slag with burned dolomite addition	AOD slag without burned dolomite addition
Below 1250	$(Mg,Mn)O \cdot Al_2O_3$ $2CaO \cdot (Fe,Mg)O \cdot 2SiO_2$ $2(Ca,Mg)O \cdot SiO_2$ **$3CaO \cdot MgO \cdot 2SiO_2$** $CaO \cdot TiO_2$	$(Mg,Mn)O \cdot Al_2O_3$ MgO $2CaO \cdot SiO_2$ **$3CaO \cdot MgO \cdot 2SiO_2$** $5CaO \cdot 4TiO_2$	MgO **$2CaO \cdot SiO_2$** $3CaO \cdot MgO \cdot 2SiO_2$ $5CaO \cdot 4TiO_2$
1250	$2CaO \cdot (Fe,Mg)O \cdot 2SiO_2$ $2(Ca,Mg)O \cdot SiO_2$ $(Al,Cr,Fe)_2O_3$ **$3CaO \cdot MgO \cdot 2SiO_2$** $CaO \cdot TiO_2$	$(Mg,Mn)O \cdot Al_2O_3$ MgO $2CaO \cdot SiO_2$ **$3CaO \cdot MgO \cdot 2SiO_2$** $5CaO \cdot 4TiO_2$	MgO **$2CaO \cdot SiO_2$** $3CaO \cdot MgO \cdot 2SiO_2$ $5CaO \cdot 4TiO_2$
1300	$2(Ca,Mg)O \cdot SiO_2$ $(Al,Cr,Fe)_2O_3$ **$3CaO \cdot MgO \cdot 2SiO_2$** $CaO \cdot TiO_2$	MgO $2CaO \cdot SiO_2$ **$3CaO \cdot MgO \cdot 2SiO_2$** $5CaO \cdot 4TiO_2$	MgO **$2CaO \cdot SiO_2$** $3CaO \cdot MgO \cdot 2SiO_2$ $5CaO \cdot 4TiO_2$
1350	$2(Ca,Mg)O \cdot SiO_2$ **$3CaO \cdot MgO \cdot 2SiO_2$** $CaO \cdot TiO_2$	MgO **$2CaO \cdot SiO_2$** $3CaO \cdot MgO \cdot 2SiO_2$ $5CaO \cdot 4TiO_2$	MgO **$2CaO \cdot SiO_2$** $3CaO \cdot MgO \cdot 2SiO_2$ $5CaO \cdot 4TiO_2$
1400	**$3CaO \cdot MgO \cdot 2SiO_2$**	MgO **$2CaO \cdot SiO_2$** $3CaO \cdot MgO \cdot 2SiO_2$ $5CaO \cdot 4TiO_2$	MgO **$2CaO \cdot SiO_2$** $3CaO \cdot MgO \cdot 2SiO_2$ $5CaO \cdot 4TiO_2$
1450	**$3CaO \cdot MgO \cdot 2SiO_2$**	MgO **$2CaO \cdot SiO_2$** $3CaO \cdot MgO \cdot 2SiO_2$	MgO **$2CaO \cdot SiO_2$** $3CaO \cdot MgO \cdot 2SiO_2$
1500	**$3CaO \cdot MgO \cdot 2SiO_2$**	MgO **$2CaO \cdot SiO_2$** $3CaO \cdot MgO \cdot 2SiO_2$	MgO **$2CaO \cdot SiO_2$**
1550	-	MgO **$2CaO \cdot SiO_2$**	MgO **$2CaO \cdot SiO_2$**
1600	-	**MgO** $2CaO \cdot SiO_2$	MgO **$2CaO \cdot SiO_2$**
1650	-	**MgO** $2CaO \cdot SiO_2$	MgO **$2CaO \cdot SiO_2$**
1700	-	**MgO**	MgO **$2CaO \cdot SiO_2$**
1750	-	**MgO**	MgO **$2CaO \cdot SiO_2$**
1800	-	**MgO**	**MgO**
Above 1800	-	**MgO**	-

Table 11. Solid phases that are formed during the solidification of AOD and CRC slags according to the experiments.

Slag (MgO+CaO)/SiO$_2$	Solid phases after cooling of the samples	SEM-image
CRC slag (1.60)	**2(Ca,Mg)O·SiO$_2$** *or* **3CaO·MgO·2SiO$_2$** (1) 2CaO·MgO·2SiO$_2$ (2) *CaO·TiO$_2$* (3)	
CRC slag with burned dolomite addition (1.86)	**3CaO·MgO·2SiO$_2$** **2CaO·SiO$_2$** 2CaO·MgO·2SiO$_2$ *MgO* *CaO·TiO$_2$*	
CRC slag with burned dolomite addition (2.18)	**2CaO·SiO$_2$** (1) **2(Ca,Mg)O·SiO$_2$** *or* **3CaO·MgO·2SiO$_2$** (2) MgO (3) *Glass phase containing Ca-, Si-, Mg- and Al-oxides* (4)	
CRC slag with burned dolomite addition (2.56)	-	
AOD slag (2.16)	**MgO** (1) 3CaO·SiO$_2$ (2)	

According to the calculations, the solidus and liquidus temperatures of the CRC slag were 1235 °C and 1485 °C, respectively. The corresponding temperatures for the AOD slag were 1440 °C and 1780 °C, respectively. Experimentally determined solidus and liquidus temperatures for the CRC slag were 1370 °C and 1442 °C, respectively. Experimentally determined solidus temperature for the AOD slag could not be accurately defined although it was noticed to be below

84

1500 °C. Experimentally determined liquidus temperature for the AOD slag was 1707 °C. Although there were considerable differences in computationally and experimentally determined solidus and liquidus temperatures, the increasing effect of burned dolomite addition on the solidus and liquidus temperatures was clearly noticeable in both considerations. In the slag protection of the converter linings, the increased solidus and liquidus temperatures are most likely to increase the amount of slag that is solidified on walls.

From Table 11 it is seen that the solidified CRC slag without the burned dolomite addition consists mainly of two oxide phases. The compositions of these phases correspond the ones of åkermanite ($2CaO \cdot MgO \cdot 2SiO_2$) and either monticellite ($2(Ca,Mg)O \cdot SiO_2$) or merwinite ($3CaO \cdot MgO \cdot 2SiO_2$). In addition to these phases there are also small amounts of an oxide containing calcium and titanium. The composition of this phase corresponds the one of perovskite ($CaO \cdot TiO_2$). According to the computations (*cf.* Table 10), the first solid phase to separate from the molten CRC slag when temperature is decreased is merwinite ($3CaO \cdot MgO \cdot 2SiO_2$) at 1500 °C followed by monticellite ($2(Ca,Mg)O \cdot SiO_2$) and perovskite ($CaO \cdot TiO_2$) at 1350 °C, corundum (Al_2O_3) at 1300 °C and finally åkermanite ($2CaO \cdot (Fe,Mg)O \cdot 2SiO_2$) at 1250 °C. In lower temperatures spinel ($(Mg,Mn)O \cdot Al_2O_3$) becomes more stable than corundum. The most significant solid phase in the solidification of CRC slag according to computations is merwinite ($3CaO \cdot MgO \cdot 2SiO_2$). It is seen that there is a good correspondence between computational and experimental results merwinite, monticellite and åkermanite being the most significant solid phases in both considerations. It is noteworthy that neither periclase (MgO) nor dicalciumsilicate ($2CaO \cdot SiO_2$) is likely to form during the solidification of the CRC slag.

The addition of burned dolomite changes the solidification behaviour of the CRC slag considerably. According to computations, the first two solid phases to separate from the molten slag when temperature is lowered are periclase (MgO) and dicalciumsilicate ($2CaO \cdot SiO_2$) neither of which was formed during the solidification of the CRC slag with no burned dolomite addition. When temperature is further decreased, merwinite ($3CaO \cdot MgO \cdot 2SiO_2$) and $5CaO \cdot 4TiO_2$ become stable as well. In temperatures below 1300 °C the amount of merwinite becomes greater than the amounts of periclase and dicalciumsilicate, and below 1250 °C some spinel is formed, too. Same solid phases could also be found in the slag samples that were studied in the experiments. Additionally, some conclusions could be made on the solidifying order of the solid phases based on the SEM-analysis of the solidified CRC slag with burned dolomite addition and with the

(MgO+CaO)/SiO_2 -ratio of 2.18. Periclase (MgO) and dicalciumsilicate (2CaO·SiO_2) appear as more or less round particles whereas the third solid phase with the composition corresponding the composition of either monticellite (2(Ca,Mg)O·SiO_2) or merwinite (3CaO·MgO·2SiO_2) is located between the periclase and dicalciumsilicate particles. This indicates that the growths of periclase and dicalciumsilicate were not limited by other solid phases, which in turn suggests that these two phases were the first two solid phases to appear in the melt and the third solid phase must have solidified afterwards. Fourth phase containing the oxides of calcium, silicon, magnesium and aluminium was also noticed in the SEM analysis. This phase represents the last remaining liquid in the system and is most likely solidified as amorphous material. In general, the solidifying orders of the CRC slag with the burned dolomite addition according to computational and experimental studies seem to be in a very good accordance with each other.

Phases that are formed during the solidification of the AOD slag are periclase (MgO) and tricalciumsilicate (3CaO·SiO_2) according to experiments and periclase (MgO), dicalciumsilicate (2CaO·SiO_2) and merwinite (3CaO·MgO·2SiO_2) according to computations.

When considering the slag protection of converter linings, the mechanical strength of the solidified slag and furthermore the durability of the slag protection are highly dependent on the composition and structure of the solid phases that are formed during the solidification. As mentioned in chapter 3.1.3, especially harmful to the slag protection is the formation of dicalciumsilicate (2CaO·SiO_2), which was detected to be formed during the solidifications of CRC slags with burned dolomite addition and during the solidification of the AOD slag.

Dicalciumsilicate exists in numerous crystalline forms and the phase transformation from β-form to γ-form can lead to a breaking of the material due to volumetric changes (Deer *et al.* 1986, Hartenstein *et al.* 1997). This means that the addition of burned dolomite into the CRC slag is not necessarily beneficial, although it elevates solidus and liquidus temperatures of the slag and therefore increases the amount of slag that is attached to the walls. However, it should be remembered that the temperature of the lining very rarely decreases so low that phase transformations with high volumetric changes occur. The risk of the phase transformation with high volumetric change is the most probable in the vicinity of tuyeres due to cooling effect of the blowing gases.

Eriksson and Björkman (2004) have also found out that by increasing the MgO content of the AOD slag with olivine and calcinated dolomite additions can

prevent the disintegration of the slag by changing the mineral composition towards to merwinite and bredigite.

6   Discussion

The goal of this thesis was to present the role of computational thermodynamics in metallurgical research and development of stainless steelmaking refining processes. More precisely, its aim was to answer how computational thermodynamics can be used to develop, optimize and understand the AOD and CRC processes by modelling the chemical reactions taking place in these processes and how computational thermodynamics may be used to connect metallurgical theory and practice in the context of stainless steelmaking.

According to Figures 1 and 2, computational thermodynamics - as well as any other tool of metallurgical R&D - can act as a link between metallurgical practice, research and education. Since CTD is supposed to have a connection to all these three aspects of metallurgy, the purpose of this chapter is to evaluate what kind of role CTD has had on metallurgical practice, research and education within the context of cases presented in this thesis and its Supplements. The role of CTD on practice (*i.e.* development in R&D) is presented in chapter 6.1 and its role on research in chapter 6.2. In addition to these, the role of CTD on education is considered in chapter 6.3 from both pedagogical and curricular perspectives. The approach presented in Figures 1 and 2 is used as a starting point in all these considerations.

6.1   Practical consequences

Computational thermodynamics was used in the research and development of AOD and CRC processes within the studies presented in the Supplements I, II, III, V and VI of this thesis. These studies focused on oxidation of silicon, carbon and chromium in the CRC process, on nitrogen solubility in stainless steels during the AOD process, on metal-slag -equilibria in the CRC process as well as on the melting and solidification behaviour of AOD and CRC slags on converter linings.

Concerning the oxidation reactions, computational thermodynamics helped to determine the order of oxidation in different process conditions. The results of calculations indicated that with high silicon contents during the early stages of the CRC process silicon is most likely to be oxidized before carbon and chromium. As the silicon content decreases below approximately 0.3-0.6 wt-%, the oxidation of carbon becomes more favourable and the carbon content of the metal begins to decrease. If the oxygen blowing is continued even further, chromium begins to oxidise excessively if the carbon content is decreased below approximately

2.5 wt-%. This means that the reduction of Cr_2O_3 from the slag is required in order to produce low carbon ferrochrome with the CRC process.

Concerning the nitrogen solubilities in stainless steels, a simplified submodel describing the influence of chromium and nickel contents of the metal as well as partial pressure of nitrogen of the gas phase on the nitrogen solubility was created based on the results of computational thermodynamics. The effects of other elements on the nitrogen solubility in a system in thermodynamic equilibrium were also considered, but based on the results of computations it was concluded that the influence of other elements is neglible within the composition and temperature range under consideration. The submodel was used as a boundary condition in the overall model that describes the nitrogen content of stainless steel in AOD process as a function of blowing time. This overall model can be used to define the optimal nitrogen-argon switch point in the production of different stainless steel grades. A delayed switch from nitrogen to argon leads to exceeded nitrogen contents in the final melt, whereas the operational costs are increased if the switch from nitrogen to argon is executed too early. Furthermore, the overall model can be utilised as a tool to study effects of individual factors like oxygen content on the nitrogen removal in an industrial AOD process.

While considering the metal-slag -reactions involving silicon, carbon and chromium, the results indicated that the oxidation reactions are not in mutual equilibrium at the end of the blowing and one should therefore be careful when veryfying thermodynamic modelling with the process measurements.

Both computational and experimental studies concerning the solidification of AOD and CRC slags showed that the increased MgO-contents achieved with burned dolomite addition had a strong increasing influence on the solidus and liquidus temperatures of the slags. In the slag protection of the converter linings, the increased solidus and liquidus temperatures are most likely to increase the amount of slag that is solidified on the walls. It was also noticed that the solid phases formed during the solidification are different with slags with and without burned dolomite addition. Especially significant is the formation of dicalciumsilicate during the solidification of slags with burned dolomite addition. In practice the appearance of dicalciumsilicate may lead to the spalling of the material due to phase transformations between its crystalline forms.

These case studies show that the use of computational thermodynamics have both direct and indirect consequences on the AOD and CRC processes and their optimization.

6.2   Consequences on research

In addition to results applicable in development of metallurgical processes presented in chapter 6.1, the cases presented within this thesis and its Supplements give a chance to consider how the use of computational thermodynamics and other methods of R&D link theory and practice and hence help to plan and execute research that is both scientifically reliable and practically relevant. Research focusing on the modelling of the AOD process is chosen here as an example through which the connecting role of methods is presented.

Analysis on the different aspects of process metallurgy presented in Figures 1-2 (*cf.* chapter 1.1) has been used to visualize the connections between the different areas of the AOD modelling. The structure of the modelling is presented in Figure 29 which is created by specifying the features presented in Figure 2 into the field of AOD modelling. Middle level of Figure 2 describing the tools of research is divided in two categories in Figure 29: the upper level represents the tools of process modelling, whereas the lower level shows the submodels that are used to model different phenomena within the considered process.
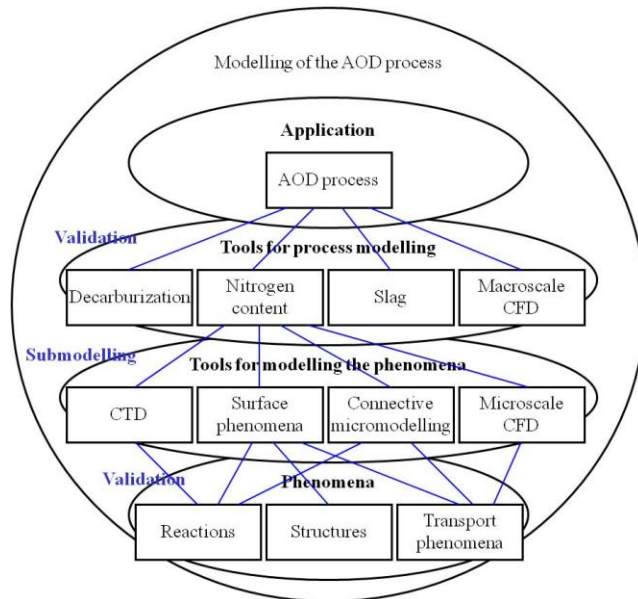

Fig. 29. Modelling of the AOD process.

All the process models presented in Figure 29 could be divided into submodels, but for the clarity's sake the connections between the two levels of modelling are only presented for the nitrogen model (*cf.* Supplement III of this thesis) which is used as an example. In order to be valid and relevant, all the process models should have connections to the application level (*i.e.* to the AOD process). On the other hand, the modelling of the phenomena should have connections to the studied phenomena that must be understood in order to be modelled properly. Validation of technological research without these connections between tools and applications as well as tools and phenomena cannot be considered as theoretically and practically relevant, since without the proper connections research will easily become detached from either practice (*i.e.* no links between tools and applications) or its scientific basis (*i.e.* no links between tools and phenomena). While validating the research, the practical relevance is verified by comparing the results of the modelling with the industrial process data that is acquired from the production of various steel grades and utilisation of various blowing practices. Proper ways for theoretical validation are either laboratory scale experiments in which the most essential phenomena are being investigated individually without disturbing factors or (if the execution of such experiments is not possible) by comparing the results of the submodels with experimental results presented in the literature.

In Figure 29, the modelling of the AOD process is divided in four more or less separate blocks that include the modelling of decarburization, nitrogen content of the steel melt, slag properties and fluid flows in the macro scale. Modelling concerning the nitrogen content of the steel melt is further divided into four submodels as is seen from Figure 29: chemical equilibria are considered in the submodel of CTD in which the equilibrium content of nitrogen in the steel melt is calculated as a function of temperature as well as steel and gas compositions (*cf.* Supplement II of this thesis for details); modelling of the surface phenomena concentrates on the behaviour of surface-active elements with a purpose to define the gas-steel-surface area through which the transfer of nitrogen can take place (*cf.* Riipi & Fabritius 2007 for details); computational fluid dynamics (CFD) is used in microscale to model the mass transfer of nitrogen in different phases and through the phase boundaries in the scale of individual gas bubbles (*cf.* Järvinen *et al.* 2008 for details) and connective micromodelling is used to combine the modelling of mass transfer and thermodynamics in order to define local equilibria in the scale of individual gas bubbles (*cf.* Järvinen *et al.* 2008 for details). The overall nitrogen model uses averaged and simplified results

of the submodels in order to create a model that can be used in the prediction of the steel melt's nitrogen content in the control of the AOD process.

As mentioned above, more detailed categorizations could be made for three other process models as well, but only nitrogen model is considered here in detail as an example. Concerning the other process models, the decarburization model includes considerations of the distribution of oxygen between the oxidising components as well as slag formation and it is used in the process control, whereas CFD is used to estimate the flows of the steel melt in the reactor scale (*cf.* Kärnä *et al.* 2008 for details). The modelling of the slag properties includes the models for viscocity as well as surface and interfacial tensions as a function of slag composition. Analogies to the nitrogen modelling have been used in order to acquire synergetic benefits.

The analysis presented in Figure 29 has pointed out several advantages for the researcher as well research manager.

From the researcher's point of view it was concluded that the visualization presented in Figure 29 helped individual researcher to outline his/her contribution as a part of a larger entity and made it easier to understand the meaning and benefits of one's own work and to plan it as a part of a wider context. The awareness of the links between one's own research and other researcher's work enabled researcher to evaluate his/her work from the less subjective and more holistic perspective and also made it easier to find a "common language" to communicate with other researchers. Based on the comments of the researchers it has been noticed that especially the researchers with scientific (*e.g.* mineralogy and chemistry) rather than engineering (*i.e.* metallurgy) background considered the use of the this analysis to be very useful in the illustration of connections between the different areas of a certain research project. It was assumed that since the applications and tools are emphasized in the engineering education, whereas the scientific education traditionally focuses mainly on the phenomena (and possibly on the methods but rarely on the applications), it is understandable that the explicit presentation of the connections between the different levels of research is more useful to the scientists than to the engineers who are used to consider problems on different levels and using different perspectives and several methods (de Vries 1996, Jenkins 1979, Korn 1994, Santander Gana & Trejo Fuentes 2006). One could conclude that the analysis in which the connections between different areas of knowledge are connected via research tools seems to be more useful for specialists than for generalists since the latter are more used to search and find the connections themselves.

A wider understanding concerning one's own work has also helped researchers to report the results of their work. Additionally, applicability and possibilities as well as lacks of the research could be considered in the wider context. From the modelling's perspective the approach has motivated researchers to create models and codes with reusable structures and hence contributed to sustainable and continuous modelling procedures. An example concerning the reusable modelling procedures is a CFD model for the emulsification of slag into the steel that was originally constructed to model the phenomena in the AOD process (*cf.* Sulasalmi *et al.* 2009 for details) and was later easily and quickly adapted for BOF, CAS-OB and ladle due to its reusable structures.

From the research manager's perspective it has been found out that the visualization helped to see the connections between different areas of research and enabled to point out the possible deficiencies of the research already during the planning. During the actual research, the visualization made it easier to see the big picture as well as to divide the research into smaller and more controllable proportions. This helped to direct the resources on the areas that are the most critical to the research as a whole. A concrete example of the advantages that has been achieved is the increased amount of scientific publications that is commonly considered to be an indicator for the quality of research (*cf.* Supplement IV of this thesis for details). Finally, the analysis has made it possible to see the connections between different research projects (*e.g.* modelling of the AOD process in comparison with the modelling of the BOF process) and thus enabled the better utilisation of competences as well as synergetic achievements.

To generalize the advantages obtained with the approach presented in Figure 29, one could conclude that analysis that takes different aspects of process metallurgy into account and which is presented graphically helps to visualize the connections between research, education and practical applications as well as the links between different areas of research or education. With the awareness of these connections, it is easier:

– to plan the research projects and to estimate the needs for personnel, competencies, *etc.* for research projects.
– to evaluate the extent of research.
– to perceive the relations between different areas of research within the same project.
– to report and to visualize the goals, methods and results of the research.
– to discuss about the role of different areas of research.

- to evaluate the validity of research.
- to present the similarities and analogies as well as differences between different research projects.
- to present and to estimate the connections between research and education.

As a conclusion for this chapter, it may be noted, that according to analyses presented in Figures 1, 2, 3 and 29, computational thermodynamics as well as other tools of metallurgical R&D are links between metallurgical theory and practice. By explicitly visualizing these connections, it is possible to achieve many advantages in research activities.

6.3   Pedagogical and curricular consequences

The purpose of engineering education is to create engineering expertise. There are various ways to define the expertise, but regardless of the criteria according to which it is defined and divided into different areas, it is essential for true expertise to include its different areas as an integrated entity. Hence it is vital to take this aim towards integrated expertise into account while planning the education and the curricula. (Collin & Tynjälä 2003, Jakobsen & Bucciarelli 2007, Katajavuori *et al.* 2006, Leinhardt *et al.* 1995, Slotte & Tynjälä 2003, Tynjälä *et al.* 1997, Tynjälä *et al.* 2003, Tynjälä *et al.* 2005) True expertise is not achieved with traditional academic education which is often plagued by so-called excessive scientification (Beder 1999, Christiansen & Rump 2008, Collin & Tynjälä 2003, Felder 1987, Jakobsen & Bucciarelli 2007, Katajavuori *et al.* 2006, Leinhardt *et al.* 1995, Rugarcia *et al.* 2000, Tynjälä *et al.* 1997, Tynjälä *et al.* 2003, Xeidakis 1994, Woods & Sawchuk 1993). It is not merely enough to create lists of intended learning outcomes, but one should also consider how to create explicit connections between theoretical and practical aspects while planning a curriculum for the engineering Master programmes (Jakobsen & Bucciarelli 2007, Tynjälä *et al.* 1997).

Since integrated education is necessary for integrated expertise, there is a need for a link that connects the different areas of expertise into an integrated entity. Approaches presented in Figures 1 and 2 create visible links between the different areas of metallurgical expertise and emphasize the role of tools and methodological expertise (*e.g.* ability to use CTD) as a link between theory and practice. The choice of methods and methodological expertise as a core content of metallurgical education is justified not only by their role in creating links between

94

theoretical and practical aspects of the discipline, but also because the different methods of research and development (experiments and analyses in addition to modelling and simulation) always have an essential role in metallurgy. Additionally, connection of theory and practice by using methodological exercises is especially important in all engineering education, because the context in which the theory is connected to technological applications (*i.e.* engineering artefacts such as metallurgical unit operations) is a key element that differentiates engineering from other sciences. It is more motivating for engineering students to have courses in which theory is not separated from the applications.

The emphasis on the methodological expertise may have its influence on the learning outcomes of the whole programme and on the goals, contents and educational methods of individual courses as well. In other words, the consequences of the approach illustrated in Figures 1 and 2 may be either pedagogical (horizontal integration) or curricular (vertical integration).

Two examples of horizontal integration that have been executed in the education of process metallugy in the programmes of process and environmental engineering at the University of Oulu, are as follows:

– Two courses of physical chemistry organized by the faculty of science were replaced with engineering oriented courses of 'Material and energy balances' (5 ECTS) and 'Thermodynamic equilibria' (5 ECTS), in which the contents were very similar to the old courses, but in which thermodynamics was not considered as a pure science, but as a tool for process design. The connection between the theories of physical chemistry and process development was obtained by choosing such teaching and assessment methods that have relevance in actual engineering work. In other words the goals of the new courses were not only to learn the fundamentals of physical chemistry, but to define chemical equilibria of the systems relevant to industrial processes and also to understand the relevance of equilibria (and their computational determination) as a part of process analysis, planning and control. So instead of lectures and terminal written exams, the new courses consist mainly of exercises and simulations that are based on authentic engineering problems. Two important features in these exercises are that:

  – the students are allowed to use the very same methods and tools that are used in real research and development (*i.e.* CTD) and
  – the problem solving is not limited to mere calculation (*i.e.* application of mathematics and chemistry), but it also contains elements in which

computationally solvable problems are created based on verbal real-life problems that in themselves are not solvable computationally.

–   In order to avoid the over-emphasis on either metallurgical processes (*e.g.* blast furnace, basic oxygen furnace, electric arc furnace, flash melting furnace) or the phenomena taking place in these processes (such as oxidation, reduction, melting, solidification, surface phenomena and so on), all the advanced courses of process metallurgy are currently based on the methodological expertise required to work as a researcher or R&D engineer within metallurgical industry. The studies consist of large courses (10 ECTS each) that are implemented as small research projects done mainly in pairs and in small groups.

The results of these changes have been excellent. All the courses in which the contents as well as teaching and assessment methods have been re-considered based on the emphasis on the methods have had passing percentages of between 92 and 97 % each year. As a comparison, in 2005 that was the last year when the old courses of physical chemistry (*cf.* above) were included in the curriculum, only 14.4 % of the students of process engineering managed to pass both courses of physical chemistry within one year of the first possibility to do so. The student feedback concerning the changes has also been very positive.

It should also be noted that the role of simulation and other methodological exercises is different in different stages of curriculum. In the beginning they can be used to illustrate different processes and phenomena in a descriptive way. One could for example use CTD and its results to examine the effects of temperature and pressure on a certain chemical reaction. Later on, these kind of exercises can be deepened by giving more emphasis on actual analytical methods that are used in process engineering: one could for example pay more attention to the rules of physical chemistry that are used in CTD and hence clarify the possibilities as well as restrictions and boundaries of the used methods. Further on, it is possible to use larger exercises of process design in which *e.g.* CTD is one tool among the others and which aim to give students more holistic view on the discipline. Finally, students should be allowed to use their skills and knowledge on the actual engineering problems in different areas of process engineering. Obviously it is possible to use analogous approach for other methods of process engineering (such as CFD) as well.

An example of the use and role of CTD during different stages of engineering curriculum is presented in Table 12.

Table 12. Role of CTD during the different stages of engineering curriculum.

Year	Nature of studies	Role of CTD
1st	Descriptive studies	Results of CTD may be used to illustrate the influence of different variables (*e.g.* temperature and pressure) on chemical reactions.
2nd - 3rd	Analytic studies	Analytic studies on rules and laws of physical chemitry required in CTD. Getting to know the possibilities and restrictions of CTD via the assumptions behind the computations.
3rd	Synthesis studies	Use of CTD as a part of larger exercises in *e.g.*process design.
4th - 5th	Advanced studies	Use of CTD to study more specific topics by using open-ended problems.
5th	Master's thesis	Use of CTD among other methods in research of a specific problem.

Although it is possible - and beneficial - to develop education by using horizontal integration on the course-level alone (as shown above), it is much more efficient to aim for true integration by building the curricular structure as well as individual courses based on links between theory and practice (*i.e.* tools and methods in metallurgy). By doing this, it is possible to achieve curricular integrity, when the connecting links of the discipline are explicitly shown.

At the University of Oulu there is no separate programme for metallurgy, since it is a part of the programmes of process and environmental engineering. In these programmes, the connecting role of tools and methods has been used when planning the curricular structure on both bachelor and master levels. The most noticeable consequences of this are the streams that connect studies from different stages of the curriculum and lead to learning outcomes that are relevant for a process engineer as well as fundamental courses that begin these streams (Hiltunen *et al.* 2011). Other implications worth mentioning are the increased role of experimental and simulation tools and methods on various courses with an aim to bring education and research closer to one another.

The learning outcomes, towards which the streams are aimed at, are chosen to correspond methodological expertise relevant to process engineers. These learning outcomes are:

- Ability for phenomena-based modelling and design (both static and dynamic simulation) in the context of process and environmental engineering (including the ability to investigate physical, chemical, biological and geoscientific phenomena).
- Ability to control industrial processes and take their technical, economic, juridic and safety issues into account.

– Ability to estimate and control the environmental impacts of industrial and community processes.
– Ability to use automation and control engineering in the context of process and environmental engineering.
– Non-technical skills that are required in engineering design, research, development and education (including e.g. social and multicultural skills).

The results from this development work indicate that the approach is suitable for comprehensive engineering education development. As mentioned above, in individual courses the proportions of students passing the courses have been high and the student feedback concerning the new approach has been positive. Although the evidence on the effects on the curricular level are much more difficult to define, it is felt that the results are best in situations in which the approach is applied on larger scale rather than individual courses.

7 Summary

The purpose of this thesis is to illustrate the role of computational thermodynamics as a part of research and development of AOD and CRC processes in the production of stainless steels. Briefly summarized, the role of CTD could be defined as essential but not adequate.

The role of CTD is essential because chemical reactions are an essential part of all metallurgical unit operations and therefore it is not possible (or at least not meaningful) to model, control and optimize these processes without taking the reactions into account. Obviously it would be possible to study the reactions via other methods, *i.e.* laboratory experiments, analyses of industrial samples and so on, but in practice CTD offers the fastest, cheapest and the most risk-free way to investigate the chemical phenomena. The biggest shortcoming of the CTD in comparison with other methods used to study the chemical reactions is a need for precise validation of the results, since the accuracy of modelling is always limited by the accuracy of used models and initial values and assumptions. The results of CTD, no matter how accurately modelled, can only be as good as the assumptions behind them. Therefore it has been - and always will be - necessary to validate the results obtained from the models with the real process data. This means that reliable modelling is only rarely achieved without an open and long-term co-operation between the modellers and the production engineers.

On the other hand, the role of CTD is not adequate since no information concerning the reaction rates can be achieved with CTD and, more importantly, chemical reactions are not the only relevant phenomena occuring in metallurgical unit operations. Despite of this, thermodynamic modelling is usually needed as a starting point for any metallurgical R&D involving chemical reactions. If the driving forces and spontaneities of reactions are not considered, it is no point in studying the rates of these phenomena either.

Within the topic of this thesis and its supplements (*i.e.* refining processes of stainless steelmaking), computational thermodynamics has been considered as a connecting link between the phenomena and the applications. Based on these considerations it is concluded that the results obtained by using CTD are not only helping to control and optimize the refining processes of stainless steelmaking, but also helping to understand how various practical process parameters and variables are linked to the phenomena occuring in these processes.

References

Andersson NÅI, Tilliander A, Jonsson LTI & Jönsson PG (2013) Investigating the Effect of Slag on Decarburization in an AOD Converter Using a Fundamental Model. Steel Research International. Vol. 84. No. 2. pp. 169-177.

Anon. (2012a) Crude steel production statistics 2001 - ISSF: International Stainless Steel Forum. Last checked: 4.3.2013. Available from: http://www.worldstainless.org/crude_steel_production/crude_2001

Anon. (2012b) Crude steel production statistics 2011 - ISSF: International Stainless Steel Forum. Last checked: 4.3.2013. Available from: http://www.worldstainless.org/crude_steel_production/crude_2011

Anon. (2012c) World Steel Association - Steel production 2011. Last checked: 4.3.2013. Available from: http://www.worldsteel.org/statistics/statistics-archive/2011-steel-production.html

Anon. (2012d) Foreign Trade Flow Stainless Steel Scrap Statistics 2011 - ISSF: International Stainless Steel Forum. Last checked: 4.3.2013. Available from: http://www.worldstainless.org/foreign_trade_stainless_scrap/foreign_trade_flow_scrap_2011

Anon. (2012e) Why is Stainless Sustainable? - Sustainable Stainless. Last checked: 4.3.2013. Available from: http://www.sustainablestainless.org/why-stainless

Bale CW, Pelton AD, Thompson WT, Eriksson G, Hack K, Chartrand P, Decterov S, Melançon J & Petersen S (2001) FactSage. Version 5.1. Software and its databases. ThermFact and GTT-Technologies.

Bale CW, Pelton AD, Thompson WT, Eriksson G, Hack K, Chartrand P, Decterov S, Melançon J & Petersen S (2006) FactSage. Version 5.4. Software and its databases. ThermFact and GTT-Technologies.

Bale CW, Pelton AD, Thompson WT, Eriksson G, Hack K, Chartrand P, Decterov S, Melançon J & Petersen S (2007) FactSage. Version 5.5. Software and its database. Thermfact and GTT-Technologies.

Ban-Ya S (1993) Mathematical Expression of Slag-Metal Reactions in Steelmaking Process by Quadratic Formalism Based on the Regular Solution Model. ISIJ International. Vol. 33. No. 1. pp. 2-11

Battle TP & Pehlke RD (1986) Kinetics of nitrogen absorption/desorption by liquid iron and iron alloys. Ironmaking and steelmaking. Vol. 13. No. 4. pp. 176-189.

Beder S (1999) Beyond technicalities: expanding engineering thinking. Journal of professional issues in engineering education and practice. Vol. 125. No. 1. pp. 12-18.

Bensaude-Vincent B & Hessenbruch A (2004) Materials science: a field about to explode? Nature materials. Vol. 3. No. 6. pp. 345-347.

Blicblau A & Bitterfeld G (1994) Relating science to engineering: employing a materials approach. European journal of engineering education. Vol. 19. No. 2. pp. 191-196.

Chipman J (1949) What is metallurgy? Metals transactions. Vol. 185. pp. 349-354.

Choulet RJ, Death FS & Dokken RN (1971) Argon-oxygen refining of stainless steel. Canadian Metallurgical Quarterly. Vol. 10. No. 2. pp. 129-136.

Choulet RJ & Masterson IF (1993) Secondary steelmaking in stainless steel refining. Iron and Steelmaker. Vol. 20. No. 6. pp. 45-54.

Christiansen FV & Rump C (2008) Three conceptions of thermodynamics: technical matrices in science and engineering. Research in science education. Vol. 38. No. 5. pp. 545-564.

Collin K & Tynjälä P (2003) Integrating theory and practice? Employees' and students' experiences of learning at work. Journal of workplace learning. Vol. 15 No. 7. pp. 338-344.

Deer WA, Howie RA & Zussman J (1986) Rock-forming minerals, Vol. IB, Disilicates and ring silicates, 2nd ed. Longman Scientific & Technical. London. 629 p.

Deo B & Boom R (1993) Fundamentals of Steelmaking Metallurgy. Prentice Hall International (UK) Limited. London, UK. 300 p.

de Vries M (1996) Technology education: beyond the "Technology is applied science" paradigm. Journal of technology education. Vol. 8. No. 1. pp. 7-15.

Eketorp S (1983) Process metallurgy - discussions of present systems and their future possibilites. Stockholm. KTH. Lectures at the Beijing University of Iron and Steel Technology. 136 p.

Eriksson J & Björkman B (2004) MgO modification of slag from stainless steelmaking. Proceeding of VII International Conference on Molten Slags, Fluxes and Salts. Cape Town, South Africa. January 25-28, 2004. pp. 455-459.

Fabritius T & Kupari P (1999) Optimization of Bottom Gas Blowing in Converter by Physical Modelling. Proceedings of SCANMET I - 1st International Conference on Process Development in Iron and Steelmaking, Volume 1. Luleå, Sweden. June 7-8, 1999. pp. 391-411.

Fabritius T, Vatanen J, Alamäki P & Härkki J (2000) Effect of sidewall blowing to the wear of the refractory lining in AOD. Proceedings of 6th Japan-Nordic countries Steel Symposium. Nagoya, Japan. November 28-29, 2000. pp. 114-121.

Fabritius T, Kupari P & Härkki J (2001a) Physical modelling of a sidewall blowing converter. Scandinavian Journal of Metallurgy. Vol. 30. No. 2. pp. 57-64.

Fabritius T, Mure P, Kupari P, Juntunen V & Härkki J (2001b) Combined blowing with three-hole lance in a sidewall blowing converter. Steel Research. Vol. 72. No. 7. pp. 237-244.

Fabritius T, Mure P & Härkki J (2003) The determination of minimum and operational gas flow rates for sidewall blowing in the AOD-converter. ISIJ International. Vol. 43. No. 8. pp. 1177-1184.

Fabritius T (2004) Modelling of combined blowing in steelmaking converters by physical models. University of Oulu. Oulu, Finland. 77 p.

Fabritius T, Kurkinen P, Mure P & Härkki J (2005) Vibration of argon-oxygen decarburisation vessel during gas injection. Ironmaking and Steelmaking. Vol. 32. No. 2. pp. 113-119.

Felder R (1987) The future ChE curriculum. Must one size fit all? Chemical engineering education. Vol. 21. No. 2. pp. 74-77.

Fruehan RJ (1976) Reaction Model for the AOD Process. Ironmaking and Steelmaking. Vol. 3. No. 3. pp. 153-158.

Ghosh S, Majumdar S, Prasad MM & Mozumdar SK (2002) Development and implementation of BOF slag splashing at Rourkela Steel Plant. Proceedings of 85th Steelmaking Conference. Nashville, Tennessee, United States. March 10-13, 2002. pp. 603-608.

Gittler P, Kickinger R, Pirker S, Fuhrmann E, Lehner J & Steins J (2000) Application of computational fluid dynamics in the development and improvement of steelmaking processes. Scandinavian Journal of Metallurgy. Vol. 29. No. 4. pp. 166-176.

Hartenstein J, Prange R & Stradtmann J (1997) Recent development of basic refractories for the stainless steel production. Proceedings of UNITECR '97 - Fifth Unified International Technical Conference on Refractories, Volume I. New Orleans, Louisiana, United States. November 4-7, 1997. pp. 295-303.

Heikkinen E-P & Fabritius T (2012) Modelling of the Refining Processes in the Production of Ferrochrome and Stainless Steel. In: Nusheh M, Ahuett Garza H & Arrambide A (eds.). Recent Researches in Metallurgical Engineering - From Extraction to Forming. InTech. 186 p. pp. 65-88. Available online: http://www.intechopen.com/articles/show/title/modelling-of-the-refining-processes-in-the-production-of-ferrochrome-and-stainless-steel

Hiltunen J, Heikkinen E-P, Jaako J & Ahola J (2011) Pedagogical basis of DAS formalism in engineering education. European journal of engineering education. Vol. 36. No. 1. pp. 75-85.

Holappa L & Taskinen P (1983) Metallurginen termodynamiikka tänään. Kemia-Kemi. Vol. 10. No. 5. pp. 387-392. [*In Finnish*]

Ito K, Amano K & Sakao H (1988) Kinetic study on nitrogen absorption and desorption of molten iron. Transactions of the iron and steel institute of Japan. Vol. 28. No. 1. pp. 41-48.

Jakobsen A & Bucciarelli L (2007) Transdisciplinary variation in engineering curricula. Problems and means for solutions. European journal of engineering education. Vol. 32. No. 3. pp. 295-301.

Janke D & Ma Z (1999) Chemische Stabilitäten von Feuerfeststoffen bei der Raffination von Stahl und Legierungsschmelzen auf Ni-Basis. Veitsch-Radex Rundschau. No. 2. pp. 61-83. [*In German.*]

Jenkins DEP (1979) The role of non-technical studies in engineering education in the first years. European journal of engineering education. Vol. 4. No. 2. pp. 119-129.

Jiang Z, Li H, Chen Z, Huang Z, Zou D & Liang L (2005) The Nitrogen Solubility in Molten Stainless Steel. Steel research international. Vol. 76. No. 10. pp. 740-745.

Jones PT (2001) Degradation mechanisms of basic refractory materials during the secondary refining of stainless steel in VOD ladles. Katholieke Universiteit Leuven. Heverlee, Belgium. 242 p.

Jung I-H, Decterov SA & Pelton AD (2004) A Thermodynamic Model for Deoxidation Equilibria in Steel. Metallurgical and Materials Transactions B. Vol. 35B. No. 4. pp. 493-508.

Järvinen M, Kärnä A & Fabritius T (2008) Detailed numerical modelling of gas-liquid and liquid-solid reactions in steel making processes. Proceedings of SCANMET III - 3rd International Conference on Process Development in Iron and Steelmaking, Volume 1. Luleå, Sweden. June 8-11, 2008. pp. 347-355.

Järvinen M, Kärnä A & Fabritius T (2009). A Detailed Single Bubble Reaction Sub-Model for AOD Process. Steel Research International. Vol. 80. No. 6. pp. 431-438.

Järvinen M, Pisilä S, Kärnä A, Ikäheimonen T, Kupari P & Fabritius T (2011) Fundamental Mathematical Model for AOD Process. Part I: Derivation of the Model. Steel Research International. Vol. 82. No. 6. pp. 650-657.

Katajavuori N, Lindblom-Ylänne S & Hirvonen J (2006) The significance of practical training in linking theoretical studies with practice. Higher education. Vol. 51. No. 3. pp. 439-464.

Kho TS, Swinbourne DR, Blanpain B, Arnout S & Langberg D (2010) Understanding stainless steelmaking through computational thermodynamics. Part 1: electric arc furnace melting. Mineral Processing and Extractive Metallurgy. Vol. 119. No. 1. pp. 1-8.

Kitamura S-Y, Okohira K & Tanaka A (1986) Influence of Bath Stirring Intensity and Top Blown Oxygen Supply Rate on Decarburization of High Chromium Molten Iron. ISIJ International. Vol. 26. No. 1. pp. 33-39.

Korn J (1994) Fundamental problems in engineering degree courses. European journal of engineering education. Vol. 19. No. 2. pp. 165-174.

Kowalski M, Spencer PJ & Neuschütz (1995) Phase diagrams. In: Allibert M, Gaye H, Geiseler J, Janke D, Keene BJ, Kirner D, Kowalski M, Lehmann J, Mills KC, Neuschütz D, Parra R, Saint-Jours C, Spencer PJ, Susa M, Tmar M & Woermann E. Slag Atlas. 2nd ed. Verlag Stahleisen GmbH. Düsseldorf, Germany. 616 p. pp. 21-214.

Krauss M, Aune RE & Seetharaman S (2004) Slag Splashing on BOF refractory linings. Steel grips. Vol. 2. No. 1. pp. 33-39.

Krivsky WA (1973) The Linde Argon-Oxygen Process for Stainless Steel; A Case Study of Major Innovation in a Basic Industry. Metallurgical Transactions. Vol. 4. No. 6. pp. 1439-1447.

Kupari P (2003) Private communication.

Kärnä A, Hekkala L, Fabritius T, Riipi J & Järvinen M (2008). CFD model for nitrogen transfer in AOD converter. Proceedings of SCANMET III - 3rd International Conference on Process Development in Iron and Steelmaking, Volume 1. Luleå, Sweden. June 8-11, 2008. pp. 155-161.

Larkimo M (1996) Romulle asetettavia vaatimuksia ruostumattoman teräksen valmistuksessa. Romun käyttö teräs- ja valimoteollisuudessa. POHTO, Oulu, Finland. November 7-8, 1996. 6 p. [*In Finnish*]

Lee J & Morita K (2003) Interfacial Kinetics of Nitrogen with Molten Iron Containing Sulfur. ISIJ International. Vol. 43. No. 1. pp. 14-19.

Lee J, Yamamoto K & Morita K (2005) Surface tension of liquid Fe-Cr-O alloys at 1823 K. Metallurgical and materials transactions B. Vol. 36B. No. 2. pp. 241-246.

Leinhardt G, McCarthy Young K & Merriman J (1995) Integrating professional knowledge: the theory of practice and the practice of theory. Learning and instruction. Vol. 5. No. 4. pp. 401-408.

Madías J, Topolevsky R, Brandaleze E, Camelli S & Bentancour M (2001) Slag-refractory adherence mechanism. Proceedings of 44th International Colloquium on Refractories - Refractories in Steelmaking. Aachen, Germany. September 26-27, 2001. pp. 36-43.

Messina CJ (1996) Slag splashing in the BOF - worldwide status, practices and results. Iron and Steel Engineer. Vol. 73. No. 5. pp. 17-19.

O'Connell J (1993) Knowledge structure: Thermodynamics. A structure for teaching and learning about much of reality. Chemical engineering education. Vol. 27. No. 2. pp. 96-101.

Ono-Nakazato H, Koyama T & Usui T (2003) Effect of Surface Concentration of Alloying Elements on Nitrogen Dissolution Rate in Molten Iron Alloys. ISIJ International. Vol. 43. No. 3. pp. 298-303.

Peaslee KD (1996) Physical modeling of slag splashing in the BOF. Iron and Steel Engineer. Vol. 73. No. 11. pp. 33-37.

Pelton A & Bale C (1986) A Modified Interaction Parameter Formalism for Non-Dilute Solutions. Metallurgical Transactions A. Vol. 17A. No. 7. pp. 1211-1215.

Rao YK & Cho WD (1990) Rate of nitrogen adsorption in molten iron-chromium alloys: Part 2 Mathematical model. Ironmaking and steelmaking. Vol. 17. No. 4. pp. 273-281.

Reck R, Chambon M, Hashimoto S & Graedel TE (2010) Global Stainless Steel Cycle Exemplifies China's Rise to Metal Dominance. Environmental Science & Technology. Vol. 44. No. 10. pp. 3940-3946.

Riekkola-Vanhanen M (1999) Finnish expert report on best available techniques in ferrochromium production, Finnish Environment Institure, Helsinki, Finland. 49 p.

Riipi J & Fabritius T (2007) Surface Tension of Liquid Fe-N-O-S Alloy. ISIJ International. Vol. 47. No. 11. pp. 1575-1584.

Roine A (2006) HSC Chemistry for Windows. Version 6.1. Software and its database. Outotec Research, Pori.

Rugarcia A, Felder R, Woods D & Stice J (2000) The future of engineering education. Part 1. A vision for a new century. Chemical engineering education. Vol. 34. No. 1. pp. 16-25.

Santander Gana MT & Trejo Fuentes LA (2006) Technology as 'a human practice with social meaning' - a new scenery for engineering education. European journal of engineering education. Vol. 31. No. 4. pp. 437-447.

Shimizu K (2001) Wear of Refractories for AOD Furnace. Journal of the Technical Association of Refractories, Japan.Vol. 21. No. 4. pp. 258-263.

Sigworth GK & Elliott JF (1974) The Thermodynamics of Liquid Dilute Iron Alloys. Metal Science. Vol. 8. No. 9. pp. 298-310.

Sjöberg P (1994) Some aspects on the scrap based production of stainless steels. Kungliga Tekniska Högskolan. Stockholm, Sweden. 157 p.

Slotte V & Tynjälä P (2003) Industry-university collaboration for continuing professional development. Journal of education and work. Vol. 16. No. 4. pp. 445-464.

Small WM & Pehlke RD (1968) The effect of alloying elements on the solubility of nitrogen in liquid iron-chromium-nickel alloys. Transactions of the Metallurgical society of AIME. Vol. 242. pp. 2501-2505.

Sulasalmi P, Kärnä A, Fabritius T & Savolainen J (2009) CFD Model for Emulsification of Slag into the Steel. ISIJ International. Vol. 49. No. 11. pp. 1661-1667.

Swinbourne DR, Kho TS, Langberg D, Blanpain B & Arnout S (2010) Understanding stainless steelmaking through computational thermodynamics. Part 2: VOD converting. Mineral Processing and Extractive Metallurgy. Vol. 119. No. 2. pp. 107-115.

Swinbourne DR, Kho TS, Blanpain B, Arnout S & Langberg D (2012) Understanding stainless steelmaking through computational thermodynamics. Part 3: AOD converting. Mineral Processing and Extractive Metallurgy. Vol. 121. No. 1. pp. 23-31.

Tang Y, Fabritius T & Härkki J (2004) Effect of fluid flows on the refractory wear in AOD. Proceedings of 3rd Metal Separation Technology Conference. Copper Mountain, Colorado, United States. June 20-24, 2004. pp. 219-226.

Taskinen P (2009) Materiaalit ja termodynamiikka. Materia. Vol. 67. No. 2. pp. 40-44. [*In Finnish*]

Tikkanen MH, Lilius K, Härkki J & Häikiö M (1984) On the Reactions of a Dolomitic Lining in the AOD Process. Scandinavian Journal of Metallurgy. Vol. 13. No. 6. pp. 371-381.

Tilliander A, Jonsson TLI & Jönsson PG (2004) Fundamental mathematical modelling of gas injection in AOD converters. ISIJ International. Vol. 44. No. 2. pp. 326-333.

Turkdogan ET (1996) Fundamentals of steelmaking. The Institute of Materials. Cambridge, UK. 331 p.

Turnock PH & Pehlke RD (1966) The solubility of nitrogen in multicomponent liquid iron alloys. Transactions of the Metallurgical society of AIME. Vol. 236. pp. 1540-1547.

Tynjälä P, Nuutinen A, Eteläpelto A, Kirjonen J & Remes P (1997) The acquisition of professional expertise - a challenge for educational research. Scandinavian journal of educational research. Vol. 41. No. 3. pp. 475-494.

Tynjälä P, Välimaa J & Sarja A (2003) Pedagogical perspectives on the relationship between higher education and working life. Higher education. Vol. 46. No. 2. pp. 147-166.

Tynjälä P, Salminen R, Sutela T, Nuutinen A & Pitkänen S (2005) Factors related to study success in engineering education. European journal of engineering education. Vol. 30. No. 2. pp. 221-231.

Virtanen E, Fabritius T & Härkki J (2004). Top lance practice for refining of high chromium melt in converter. Proceedings of SCANMET II - 2nd International Conference on Process Development in Iron and Steelmaking, Volume 2. Luleå, Sweden. June 6-8, 2004. pp. 155-164.

Visuri V-V, Järvinen M, Sulasalmi P, Heikkinen E-P, Savolainen J & Fabritius T (2013a) A mathematical model for the reduction stage of the AOD process. Part I: Derivation of the model. ISIJ International. Vol. 53. No. 4. pp. 603-612.

Visuri V-V, Järvinen M, Savolainen J, Sulasalmi P, Heikkinen E-P & Fabritius T (2013b) A mathematical model for the reduction stage of the AOD process. Part II: Model validation and results. ISIJ International. Vol. 53. No. 4. pp. 613-621.

Wei J-H & Zhu D-P (2002) Mathematical Modeling of the Argon-Oxygen Decarburization Refining Process of Stainless Steel: Part I. Mathematical Model of the Process. Metallurgical and Materials Transactions B. Vol. 33B. No. 1. pp. 111-119.

Wei J-H, Cao Y, Zhu H-L & Chi H-B (2011) Mathematical Modeling Study on Combined Side and Top Blowing AOD Refining Process of Stainless Steel. ISIJ International. Vol. 51. No. 3. pp. 365-374.

Wijk O (1992) Stainless steelmaking in converters. In: Engh TA: Principles of Metal Refining. Oxford University Press. Oxford, United Kingdom. 473 p. pp. 281-301.

Woods D & Sawchuk R (1993) Knowledge structure: Fundamentals of chemical engineering. Chemical engineering education. Vol. 27. No. 2. pp. 80-85.

Wranglén G (1985) An Introduction to Corrosion and Protection of Metals. Chapman and Hall. New York, USA. 288 p.

Xeidakis G (1994) Engineering education today: the need for basics or specialization. European journal of engineering education. Vol. 19. No. 4. pp. 485-501.

Xiao Y, Holappa L & Reuter MA (2002) Oxidation State and Activities of Chromium Oxides in $CaO-SiO_2-CrO_x$ Slag System. Metallurgical and Materials Transactions B. Vol. 33B. No. 4. pp. 595-603.

Zhu H-L. Wei J-H. Shi G-M. Shu J-H. Jiang Q-Y & Chi H-B (2007) Preliminary Investigation of Mathematical Modeling of Stainless Steelmaking in an AOD Converter: Mathematical Model of the Process. Steel Research International. Vol. 78. No. 4. pp. 305−310.